REDUCTION OF OFFSHORE PLATFORM RESPONSE WITH A LIQUID VIBRATION ABSORBER AND SEISMIC RESPONSE OF ELEVATED LIQUID STORAGE TANKS

SENG CHEOK LEE

REDUCTION OF OFFSHORE PLATFORM RESPONSE WITH A LIQUID VIBRATION ABSORBER

and

SEISMIC RESPONSE OF ELEVATED LIQUID STORAGE TANKS

by

Seng Cheok Lee, B.Sc.(C.Eng) ©

A Thesis submitted in partial fulfillment
of the requirements for the degree of
Master of Engineering

Faculty of Engineering and Applied Science
Memorial University of Newfoundland

August 1979

St. John's Newfoundland, Canada

Author

Seng Cheok Lee

Approved by :

Supervisor

D. V. Reddy

Dr. D. V. Reddy, Professor
Faculty of Engineering and
Applied Science

Internal Examiner

External Examiner

To My Family

ABSTRACT

The thesis is divided into two parts - I and II.

I Reduction of Offshore Platform Response with a Liquid Vibration Absorber

The LVA consists of a liquid-filled cylindrical container mounted near the deck level of the platform. During wave excitation, the liquid in the container swirls into an oscillating motion which interacts with the platform motion to produce a reduction in the platform response. The reduction in the platform response is largely due to energy dissipation through damping of the liquid, and to a smaller extent the inertia of the liquid. In this investigation, the effectiveness of the LVA in reducing the dynamic response of the offshore platform model is studied. The finite element programme for dynamic analysis of two-dimensional fixed offshore platforms, developed by DuVall (1), has been extended by Glacel (2) to include damping effects and a tuned mass damper. This study describes further modifications of the work with an additional option of replacing the actual spring mass model by an LVA. The relatively rigid container wall is discretised by finite beam elements. The work of Housner (3) is employed to account for the liquid sloshing loads on the container wall, while the liquid damping is based on a semi-empirical formulation by Stephens et al (4). The structural response of the model is determined for a digitised wave height spectrum, with and without the LVA in operation. The platform is analysed to determine the LVA effectiveness, and the variation of the system response with the LVA parameters. The various parameters considered are, cylinder radius,

liquid height, liquid mass, frequency, and damping. Methods of frequency tuning, and damping device mechanisms are discussed.

II Seismic Response of Elevated Liquid Storage Tanks

The structure under consideration consists of a liquid storage tank mounted on an axisymmetric pedestal. The tank is a thin elastic cylinder with an axisymmetric dome-top and a conical base which is relatively rigid. A finite element model is presented for the seismic analysis of the structure. The shell mass and stiffness matrices are generated by using the computer code SAMMSOR-II (56). The procedure of Shaaban and Nash (45) is used to generate the added liquid mass matrix which accounts for the hydrodynamic effect on the tank wall. A digitised acceleration of an earthquake is provided as the ground excitation input, and the displacement response of the whole system determined by mode superposition.

ACKNOWLEDGEMENTS

The author is very thankful to his supervisor, Professor D. V. Reddy, for his excellent guidance, valuable suggestions and encouragement at every stage of the thesis. Appreciation is expressed to Dr. M. Arockiasamy and Dr. W. Bobby for valuable ideas and enthusiastic support. The encouragement of Dean Dempster, Faculty of Engineering and Applied Science, and Dean Aldrich, School of Graduate Studies, is gratefully acknowledged. Special thanks are due to Gary Somerton for his help in the computing work. The graduate fellowship award by the University, and the partial support by the Natural Sciences and Engineering Research Council Canada under Grant No. 85619 of Dr. D. V. Reddy are gratefully acknowledged.

TABLE OF CONTENTS

LIST OF TABLES

LIST OF FIGURES

NOTATION

Part One

$\underline{CV}$	Rayleigh viscous damping matrix
$\underline{CH}$	Hysteretic damping matrix
C_I	Inertial coefficient
c_a	Absorber damping
D	Diameter of structural member
d	Depth of liquid in cylindrical container
E	Young's modulus
$E(\eta^2)$	Mean square of wave amplitude
f	Ratio of absorber frequency to platform frequency
g	Gravitational acceleration
$\bar{g}$	Ratio of wave frequency to platform frequency
H	Wave height from tip to trough
H_0	Height of mass, M_0, from the cylinder base
H_1	Height of mass, M_1, from the cylinder base
h	Water depth from ocean floor to still water surface
$I(\xi)$	Moment of inertia at an arbitrary point along the element
$\underline{K}$	Stiffness matrix
$\underline{KG}$	Geometric stiffness matrix
k_a	Absorber spring stiffness constant
k_{ij}	Elements of stiffness matrix, $\underline{K}$
kg_{ij}	Elements of geometric stiffness matrix, $\underline{KG}$
M	Main mass of a two DOF structural system
M	Total liquid mass in cylindrical container
$\underline{M}$	Mass matrix

M_0	Impulsive mass of fluid in a cylindrical container
M_1	Convective mass of fluid in a cylindrical container
$N(\xi)$	Axial force at an arbitrary point along the element due to the dead loads above that point
$\underline{P}$	Wave load vector
R	Radius of cylindrical container
r	Pile radius
$S(\omega)$	Wave spectral density
s	Depth of baffle below mean free surface level
t	Time in seconds
u	Fluid particle velocity
w	Baffle width
$\underline{x}$	Displacement vector
x_{st}	Static displacement of main mass in a two DOF system
z	Upward vertical distance from the seabed
$\bar{z}$	Amplitude of sloshing liquid at tank wall
D	Flexural plate rigidity
λ	Wave length
σ^2	Variance of wave amplitude
σ_o	Standard deviation of deck displacement without the LVA
σ_x	Standard deviation of deck displacement with LVA
σ_n	Normalised standard deviation of deck displacement, σ_x/σ_o
ω, Ω	Wave Frequency
ω_a	Absorber frequency, or frequency of sloshing liquid
ω_s	Fundamental frequency of offshore platform
ν	Kinematic viscosity
ν	Poisson's ratio

α,β	Viscous damping coefficients
γ	Hysteretic damping coefficient
ξ	Liquid damping ratio
ξ_a	Damping ratio of absorber
η	Wave amplitude
ρ	Density of liquid
ρ_m	Mass per unit area of membrane
ρ_p	Density of plate material
μ	Mass ratio, $\rho\pi R^2 d/M$
τ	Tensile force per unit length of membrane

Part Two

$\underline{A}$	Added mass matrix accounting for hydrodynamic effect
a_0,a_1	Rayleigh damping coefficients
$\underline{C}$	Damping matrix
d	Liquid depth
E	Young's modulus
$\underline{F}_g$	Foundation force vector
f_y	Structural yield stress
g	Gravitational acceleration
I	Section modulus
H	Liquid depth
$\underline{K}$	Overall stiffness matrix for the elevated tank system
$\underline{K}_f$	Liquid stiffness matrix
$\underline{K}_s$	Shell stiffness matrix
M_{cr}	Critical buckling moment

$\underline{M}$	Overall mass matrix for the elevated tank system
$\underline{M}_f$	Liquid mass matrix
$\underline{M}_s$	Shell mass matrix
$M_s, M_\theta, M_{s\theta}$	Stress couples
$N_s, N_\theta, N_{s\theta}$	Stress resultants
p	Liquid pressure
$\underline{P}$	Liquid element nodal pressure
$\underline{P}_{eff}$	Effective force vector
R	Cylinder radius
$\underline{S}$	Coupling force matrix
T	Kinetic energy of liquid
t	Time in seconds
t	Cylinder thickness
$\underline{U}$	Shell nodal displacement vector
u	Shell displacement in meridional direction
v	Shell displacement in circumferential direction
$\bar{V}$	Velocity vector of liquid
W	Work done on liquid
w	Shell displacement in radial direction
$\underline{Y}$	Generalised displacement vector
z	Upward vertical distance from the mean free surface level
∇	Laplacian operator
ϕ	Velocity potential of liquid
$\underline{\phi}$	Mode shape vector
ρ	Liquid density
ω	Frequency of the liquid-filled elevated tank
ξ	Damping ratio of the liquid-filled elevated tank

PART ONE

REDUCTION OF OFFSHORE PLATFORM RESPONSE WITH A LIQUID VIBRATION ABSORBER

CHAPTER 1

INTRODUCTION

It has become a necessary guideline that the fundamental frequency of the offshore platform be no less than 0.2 Hz owing to the fact that waves in the frequency range below this value have the greatest energy content. To satisfy this condition, more structural material is required, consequently increasing the cost of the platform. A possible solution of reducing the offshore platform response with considerably less cost is to install a tuned mass damper near the deck level. The tuned mass damper, whose function is to absorb energy is essentially a spring-mass-dashpot system. When suitably damped, it can be an effective device in reducing the dynamic response of the platform. The tuned mass damper has proven to be successful for tall buildings in reducing the structural response to wind excitation. The extension of the tuned mass damper concept to an offshore platform was investigated by Glacel (2); analysis of the effectiveness of the mass damper indicated a considerable reduction in the platform response to wave loading. One setback to the use of the tuned mass damper is that a reduction of the platform response is achieved at the expense of large deflections and stresses in the damper spring. More important is the fact that a large free travel space required by the damper on the overcrowded platform can be expensive in terms of space. It is suggested that an alternative for the application of the mass damper concept is the use of a liquid vibration absorber (LVA). It is expected that the LVA will be less costly to install and maintain than the actual spring-mass damper.

The main advantage of the LVA over the actual spring-mass damper is that the amplitude of the latter is in the horizontal direction, while that of the former is in the vertical direction, overcoming large horizontal space requirements.

CHAPTER 2

LITERATURE REVIEW

The topics reviewed are the wave amplitude spectrum, analysis of wave forces on structures, response analysis of offshore structures to ice forces, and the application of the tuned mass damper concept in civil engineering.

2.1 Wave Force Analysis

Several wave theories have been developed, depending on the sea conditions. In relatively deep water, Stoke's Fifth Order theory described by Skjelbreia and Hendrickson (5) is commonly used to describe steep nonlinear waves. It has been found in deep waters, that predictions of water particle velocities and acceleration using Airy Linear theory, but with integration of the forces up to the actual water surface, give results which do not differ greatly from predictions based on Stoke's Fifth Order theory.

For determination of wave forces, the Morison equation is sufficient for structural members of relatively small diameter - $D/\lambda < 0.2$, provided there is no wave scattering due to the local influence of neighbouring components. The evaluation of the inertial force term in the Morison equation requires the inertial coefficient, C_I, for the particular structural component shape and the corresponding direction of the acceleration vector. Values of C_I for various simple geometrical shapes have been given by Myers et al (6). The drag force coefficient, C_D, was recommended as 0.6 by Evans (7) and Hudspeth (8) for data obtained from the Gulf of Mexico. For slender structural members in deep waters, the drag force may be omitted without losing significant accuracy.

2.2 Wave Spectrum

The sea water surface is commonly described as a stationary, ergodic Gaussian, or normal process with zero mean (9). This process can be described by representing the sea at any place and time by the wave spectrum $S(\omega)$ which has the property

$$\sigma^2 = E(\eta^2) = 2 \int_0^{\infty} S(\omega)d\omega \tag{2.1}$$

where

$S(\omega)$ = wave spectrum in m^2-s,

σ^2 = variance of wave amplitude,

and

$E(\eta^2)$ = mean square of wave amplitude.

Several empirical derived wave spectra representing the sea conditions are available. The Pierson-Moskowitz (10), which is the most widely used, is given by

$$S(\omega) = \left(\frac{g^2\alpha_s}{\omega^5}\right) e^{-\beta(\omega'/\omega)^4} \tag{2.2}$$

where

$g = 9.81$ m/s^2,

$\alpha_s = 8.1 \times 10^{-3}$,

$\beta = 0.74$,

$\omega' = g/u$,

and

u = windspeed in m/s.

The P-M spectrum used in this work corresponds to seas generated by

120 km/hr storms.

2.3 Ice Forces on Structures

Although not within the scope of the thesis, an environmental loading of particular concern to the expanding interests on offshore oil industry in Newfoundland is that due to moving ice.

Comprehensive studies were carried out during the period 1930 - 60 by Korzhavin (11) and Zubov (12) for the determination of ice pressures on structures in rivers. Blenkarn and Knapp (13) discussed the ice conditions and maximum ice forces in the Grand Banks off the coast of Newfoundland. Kopaigorodski et al (14) made model studies to determine the mean ice pressures and variation of the values around the means, and concluded that sheets with small h/d (i.e. thickness to indentor width) ratios fail by instability while shear failures occur for sheets with large h/d ratios.

The dynamic response of an offshore monopod at Cook Inlet, Alaska, subjected to current-driven ice loads for dynamic response has been studied by Blumberg and Strader (15). Reddy, Cheema and Swamidas (16) developed response spectra for ice forces and used these for analysing the response analysis of a framed tower taking into account the three-dimensionality. Swamidas and Reddy (17) analysed an offshore monopod tower considering ice-stucture interaction by the finite element method. A detailed literature review on the development of ice engineering is well described in Ref. 16.

2.4 Application of the Tuned Mass Damper Concept

Literature on the study of a vibration absorber dates back to 1909, when Fahm advocated the absorber to reduce the dynamic motions of ships (18). The motion of the main system is reduced when the inertial force of the absorber interacts with the exciting force. In addition to reducing the motion of the main mass by its inertial effects, it also reduces the system response by acting as an energy dissipating device when provided with adequate damping. Morrow et al (19) showed that, under a white noise input the absolute displacement of the mass could be reduced with an absorber of adequate damping. Gupta and Chandrasekaran (20) studied the use of absorbers to limit structural response to earthquake excitations. Wirsching and Yao (21) developed analogue computer simulations of structures with absorbers, subjected to non-stationary earthquake-like excitations, and indicated reduction in internal loads for certain multistorey structures. Crandall and Mark (22) analysed a single-degree-of-freedom system subjected to a white noise base acceleration. Wirsching and Campbell (23) generalised their study to a multi-degree -of-freedom system and optimised the absorber parameters to minimise the relative motions of the system. McNamara (24) studied the application of the tuned mass damper to reduce wind-induced structural response of buildings for an elastic range, and obtained the response reductions for various damper parameters. In a study on the TMD application to offshore platforms, Glacel (2), reported significant reduction in the platform response, and an increase in fatigue life of steel-jacketed platforms.

CHAPTER 3

THEORETICAL FORMULATION

3.1 The Offshore Platform

The offshore platform considered in the analysis is an axisymmetric tower with the base fixed to the ocean bed, and supporting a load representing the deck, as shown in Fig. 3.1. The matrix equation which is used to model the dynamic motions of the platform in response to wave forces is

$$\underline{M}\,\ddot{\underline{x}} + [\,\underline{K} + \underline{KG}\,]\,\underline{x} = \underline{P}\,(z,x,t) \tag{3.1}$$

where $\underline{M}$, $\underline{K}$, and $\underline{KG}$ are the mass, stiffness, and geometric stiffness matrices, and $\underline{P}$ represents the vector of wave loads imposed on the structure. The finite element programme of Ref. 1, which is used to analyse the dynamic response of the offshore platform described above, is based on the formulation of two-dimensional beam elements.

3.2 Beam Element

Consider a non-uniform straight beam segment as shown in Fig. 3.2 having two degrees of freedom at each node, horizontal translation (x_1,x_3) and rotation (x_2,x_4). The displacement functions chosen, satisfying the nodal and internal continuity requirements are the cubic hermitian polynomials given as:

$$x = \psi_1(\xi)x_1 + \psi_2(\xi)x_2 + \psi_3(\xi)x_3 + \psi_4(\xi)x_4 \tag{3.2}$$

where

$$\psi_1(\xi) = 1 - 3\xi^2 + 2\xi^3, \tag{3.3a}$$

$$\psi_2(\xi) = 3\xi^2 - 2\xi^3, \tag{3.3b}$$

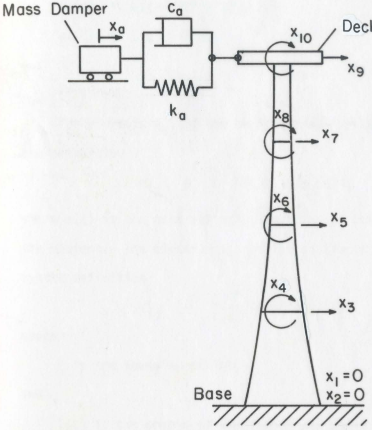

Fig. 3.1 Fixed Offshore Platform
with a Tuned Mass Damper

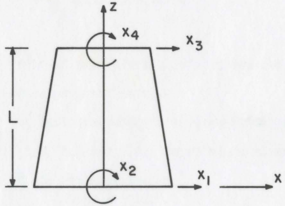

Fig. 3.2 Beam Element

$$\psi_3(\xi) = L(\xi - 2\xi^2 + \xi^3), \tag{3.3c}$$

$$\psi_4(\xi) = L(\xi^3 - \xi^2), \tag{3.3d}$$

and

$$\xi = z/L \tag{3.3e}$$

The elements m_{ij} of the mass matrix, $\underline{M}$, are determined from the definition

$$m_{ij} = L\int_0^\infty m(\xi)\psi_i(\xi)\psi_j(\xi)d\xi \tag{3.4}$$

where $m(\xi)$ is the mass per unit length at an arbitrary point along the element. The elements k_{ij} of the stiffness matrix, $\underline{K}$, are given by the definition

$$k_{ij} = \frac{E}{L}\int_0^\infty I(\xi)\psi_i''(\xi)\psi_j''(\xi)d\xi \tag{3.5}$$

where

E is the Young's modulus,

and

$I(\xi)$ is the moment of inertia at any point along the element.

The elements k_{ij} of the geometric stiffness matrix, $\underline{KG}$, are given by the definition

$$kg_{ij} = \frac{1}{L}\int_0^\infty N(\xi)\psi_i'(\xi)\psi_j'(\xi)d\xi \tag{3.6}$$

where

$N(\xi)$ is the axial force at an arbitrary point along the element due to the dead loads above that point.

A five-point scheme of the Gaussian quadrature integration is used to obtain the terms of Eqs. 3.4, 3.5 and 3.6. Detailed formulation of the matrices $\underline{M}$, $\underline{K}$, and $\underline{KG}$ is given by Ref. 1.

3.3 Damped Equations of Motion

If structural damping is considered, Eq. 3.1 becomes

$$\underline{M}\,\ddot{\underline{x}} + \underline{CV}\,\dot{\underline{x}} + [\,\underline{CH} + [\underline{K} + \underline{KG}]\,]\underline{x} = \underline{P} \qquad (3.7)$$

where

$$\underset{\text{Rayleigh Viscous Damping}}{\underline{CV}} = \alpha\underline{M} + \beta\underline{K} \qquad (3.8)$$

in which α and β are the viscous damping coefficients, and

$$\underset{\text{Hysteretic Damping}}{\underline{CH}} = i2\gamma[\underline{K} + \underline{KG}] \qquad (3.9)$$

in which γ is the hysteretic damping coefficient

Replacing $[\underline{K} + \underline{KG}]$ by $\underline{K}$, Eq. 3.7 becomes

$$\underline{M}\,\ddot{\underline{x}} + [\alpha\underline{M} + \beta\underline{K}]\dot{\underline{x}} + (1 + i2\gamma)\underline{K}\,\underline{x} = \underline{P} \qquad (3.10)$$

3.4 Wave Forces

From Airy's wave theory the fluid particle acceleration, $\frac{du}{dt}$, is given by

$$\frac{du}{dt} = \frac{1}{2}H\omega^2\frac{\cosh(kz)}{\sinh(kh)}e^{i\omega t}, \qquad (3.11)$$

where

H = wave height from tip to trough,

k = wave number, $k=2\pi/\lambda$,

λ = wave length,

h = water depth from ocean floor to still water surface,

z = distance from ocean floor upwards,

and

$\omega^2 = kg\tanh(kh)$.

The Morison equation is used to obtain the loads imposed by ocean waves on the platform. For deep waters, the drag force term is omitted, and the horizontal force $dP(z)$ on a differential length of a single pile, dz, is given by

$$dP(z) = C_I \rho \pi r^2 \frac{du}{dt} dz \qquad (3.12)$$

where

C_I = inertial coefficient,

ρ = density of water,

and

r = pile radius.

The total wave force on the pile between two points z_1 and z_2, where $z_1 < z_2 < z_{surface}$ is given by

$$P = \int_{z_1}^{z_2} dP$$

$$= \int_{z_1}^{z_2} \left(C_I \rho \pi r^2 \frac{du}{dt} \right) dz \qquad (3.13)$$

3.5 Determination of Platform Response

The displacement vector $\underline{x}$ of the platform can be defined as

$$\underline{x} = \underline{A}\,\underline{P}\,, \qquad (3.14)$$

where

$\underline{A}$ is a coefficient matrix to be determined,

and

$\underline{P}$ is the wave load vector, as defined in 3.1.

Observing the nature of Eqs. 3.11 and 3.13, $\underline{P}$ can be written as $\underline{P}e^{i\omega t}$, and Eq. 3.10 gives

$$(-\omega^2 \underline{M} + i\alpha\omega \underline{M} + \underline{K} + i2\gamma \underline{K} + i\omega\beta \underline{K})\underline{A}\,\underline{P}e^{i\omega t} = \underline{P}e^{i\omega t} \qquad (3.15)$$

and

$$\underline{A} = [-\omega^2\underline{M} + i\alpha\omega\underline{M} + \underline{K} + i2\gamma\underline{K} + i\omega\beta\underline{K}]^{-1} \tag{3.16}$$

A set of vectors, $P(\omega_i)$, can be obtained from a set of wave amplitudes , $H(\omega_i)$, which is used to excite the structural model. Consequently, the corresponding set of displacement vectors, $\underline{x}(\omega_i)$ are obtained from Eq. 3.14.

3.6 Wave Amplitude Spectrum

$H(\omega_i)$ may be obtained from a condensed spectrum represented by a finite number of wave frequencies, ω_i. This condensed spectrum is obtained by determining the area between ω-$d\omega$ and ω+$d\omega$ of the Pierson -Moskowitz wave energy spectrum (as shown in Fig. 3.3a) around a specified frequency ω, taking the square root of that area, and assigning that value to the frequency. This is done for all frequencies specified, forming a histogram of frequencies, ω_i, versus the equivalent wave amplitudes, η_i, as shown in Fig. 3.3b. The variance of the wave amplitudes can be represented by the sum of the squares of the discretised wave amplitudes,

$$\sigma^2 = \sum_{i=1}^{N} (\eta(\omega_i))^2 , \tag{3.17}$$

where N is the total number of discretised wave amplitudes.

3.7 Modelling of the LVA

The method of modelling the sloshing loads of a liquid with a free surface in an accelerating container, (Fig. 3.4a), developed by Ref. 3, is used in this study. When a container containing a liquid of mass M is accelerated in a horizontal direction, a certain fraction of the liquid is forced to participate in this motion as if

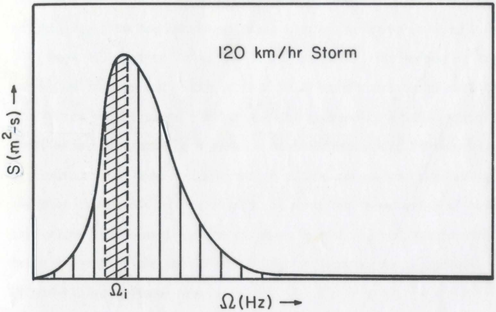

Fig. 3.3a Pierson-Moskowitz Wave Energy Spectrum

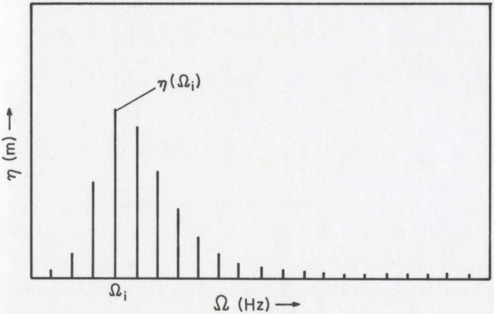

Fig. 3.3b Discretised Wave Amplitude

it were a solid mass, M_0, that is rigidly attached to the tank at a height, H_0, from the bottom of the container as shown in Fig. 3.4b. This mass is referred to as the impulsive mass. The motion of the tank also induces oscillations into the liquid exerting an oscillating force on the tank, similar to that exerted by a solid mass, M_1, oscillating horizontally against a restraining spring as shown in Fig. 3.4b. This mass is referred to as the convective mass since it involves the motion of the liquid. A detailed formulation of the equivalent spring-mass system is given by Ref. 3, and the resulting terms expressing the mechanism of liquid sloshing in an upright liquid-filled cylinder are

$$M_0 = \frac{1}{\sqrt{3}} M \left(\frac{d}{R} \right) \left(\tanh\left(\sqrt{3}\,\frac{R}{d}\right) \right), \tag{3.18a}$$

$$H_0 = \frac{3}{8} d \left(1 + \frac{4}{3}\left(\left(\sqrt{3}\,\frac{R}{d}\right)/\tanh\left(\sqrt{3}\,\frac{R}{d}\right) - 1 \right) \right), \tag{3.18b}$$

$$M_1 = M \frac{1}{4} \left(\frac{11}{12}\right)^2 \sqrt{\frac{27}{8}}\,\frac{R}{d} \tanh\left(\sqrt{\frac{27}{8}}\,\frac{d}{R}\right), \tag{3.18c}$$

$$H_1 = d \left(1 - \left(\cosh\left(\sqrt{\frac{27}{8}}\,\frac{d}{R}\right) - \frac{135}{88}\right) / \left(\sqrt{\frac{27}{8}}\,\frac{d}{R} \sinh\left(\sqrt{\frac{27}{8}}\,\frac{d}{R}\right) \right) \right), \tag{3.18d}$$

and

$$\omega^2 = \frac{g}{R}\sqrt{\frac{27}{8}} \tanh\left(\sqrt{\frac{27}{8}}\,\frac{d}{R}\right) \tag{3.18e}$$

where

ω = fundamental sloshing frequency,

and

M_0, H_0, M_1, H_1, R and d are defined in Fig. 3.4.

These expressions include fluid pressures on the bottom of the container. Although expressions used by Ref. 3 involved some approximations, the results given by his theory were shown to be within 2.5 % of the classical theory, and considered sufficiently accurate for the present investigation.

3.8 Damping of Sloshing Liquids

Viscous damping of sloshing liquids is associated with the dissipation of energy during oscillations, resulting in the decrease in the amplitude of successive oscillations. This decreasing amplitude can be described by the damping ratio as

$$\xi = \frac{1}{2\pi} \frac{\text{Amplitude of any oscillation}}{\text{Amplitude one cycle later}} \tag{3.19}$$

Viscous damping depends on the container radius, R, liquid depth, d, and kinematic viscosity, ν. Owing to the fact that liquid sloshing is essentially a nonlinear phenomenon, few theories are available for predicting the damping of liquid motion in a cylinder. A semi-empirical equation for evaluating the damping ratio of a liquid in a cylindrical container was obtained by Ref. 4, and given as

$$\xi = 0.56\nu^{1/2} R^{-3/4} g^{-1/4} \tanh(1.84 \frac{d}{R}) (1 + 2(1 - \frac{d}{R})\operatorname{csch}(3.68 \frac{d}{R})) \tag{3.20}$$

The damping ratios of a few liquids based on Eq. 3.20 are given in Table 3.1. A few liquids have relatively high kinematic viscosities, giving ξ_a (for the same cylinder geometry and liquid depth) as high as 1 %, but the practicability of using them is not known.

Table 3.1 Damping Ratio of Liquids

Liquid	Cyl. Radius R	Liquid Depth d	Kin. Viscosity ν at 10° C	Damp. Ratio ξ at 10° C
Water	6 m	1.6 m	$1 \times 10^{-6} m^2/s$	0.0001
Glycerin	6 m	1.6 m	$3 \times 10^{-3} m^2/s$	0.005

3.9 The Absorber Cylinder

The cylinder is divided into two finite beam elements with lengths depending on H_0 and H_1 as shown in Fig. 3.5a,b. When the liquid-filled cylinder is mounted on the offshore platform, five additional degrees of freedom, x_1', x_2', x_3', x_4', and x_a, as shown in Fig. 3.4b, are added. The response of the cylinder wall, does not have any significant effect on the dynamic motion of the platform. Hence, the flexibility of the cylinder wall need not be considered.

3.10 Relation of Liquid Mass and Frequency with Cylinder Geometry

The sloshing frequency of a liquid in a cylinder depends on the radius, R, and the ratio, d/R. Fig. 3.6, which is based on Eq. 3.18, shows two sets of curves, one joining the coordinates ($\frac{d}{R}$, R) corresponding to the same sloshing frequencies, and the other corresponding to the same total liquid mass in the cylinder. For the range of values $0 < \frac{d}{R} < 0.9$, an increase in the sloshing frequency, ω_a, is predominantly due to an increase in d/R, while for the range $\frac{d}{R} > 0.9$, the increase is predominantly due to a decrease in the radius, R. Fig. 3.6 will be used later in the analyses for variation of absorber parameters.

Fig. 3.7 shows the M_0/M and M_1/M values for varying d/R values. It can be seen from the figure that M_0/M increases with increasing d/R, while M_1/M decreases. The value M_1/M is of some significance, as it corresponds to the oscillating mass of the vibration absorber. It may be advantageous, therefore, to choose a suitable d/R ratio in order to provide a larger convective (or oscillating) mass M_1, but a change in d/R ratio can affect other parameters; for example, if the

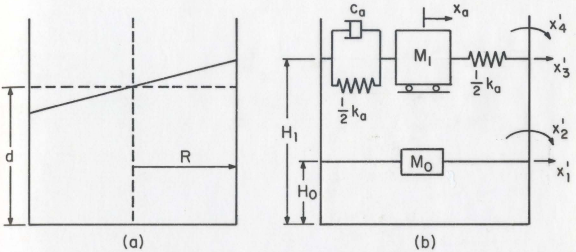

Fig. 3.4 Housner's Theory. a) Liquid-Filled Cylinder b) Equivalent Mechanical System

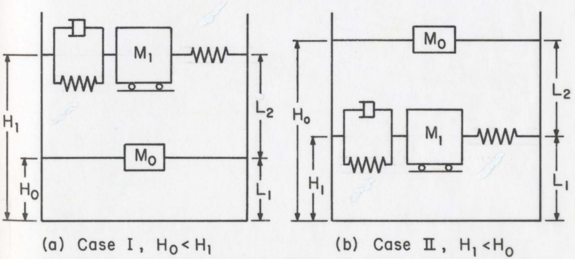

Fig. 3.5 Cases of Mechanical Systems

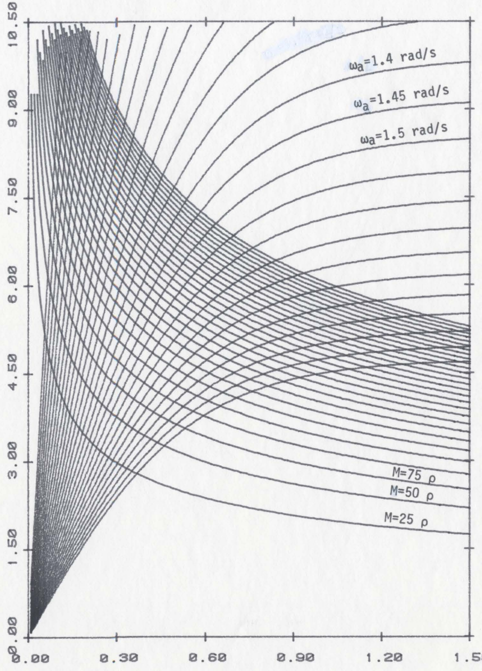

Fig. 3.6 Mass-Frequency-Dimension Chart

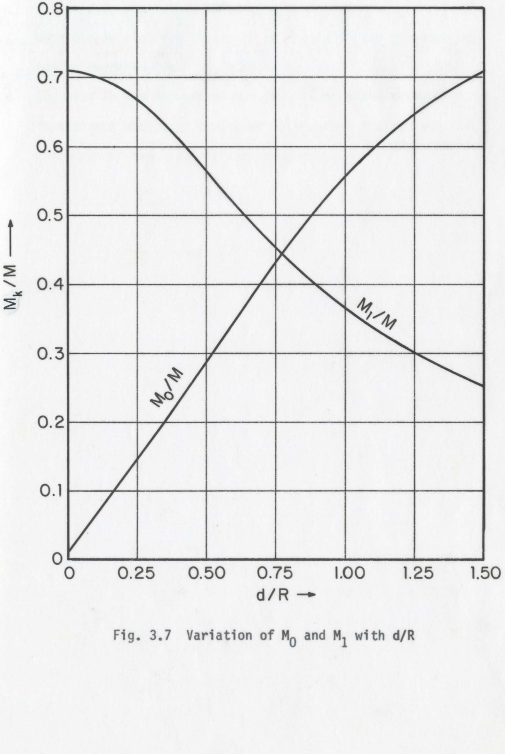

Fig. 3.7 Variation of M_0 and M_1 with d/R

liquid mass is kept constant and d/R reduced by a certain amount, three parameters are affected :

a) Increase in convective mass, M_1,

b) Decrease in sloshing frequency of liquid in the cylinder (as can be inferred from Fig. 3.6),

c) Decrease in the impulsive mass, M_0, causing an increase in the deck mass, and consequently reducing the fundamental frequency of the platform very slightly.

CHAPTER 4

APPLICATION OF LVA TO AN OFFSHORE PLATFORM

4.1 Offshore Platform Response without an Absorber

The 366 m offshore platform of Ref. 2 is used as a model in this analysis, the fundamental frequency of which is 0.2 Hz. For convenience, the structural data of the platform are shown in Table 4.1. The model is first excited without the absorber by wave loading obtained from the discretized Pierson-Moskowitz wave energy spectrum (correponding to 120 km/hr storm). The output is given as a series of steady-state displacements, rotation, acceleration at each nodal point, and strain at the midpoint of each element. Curve A of Fig. 4.1 gives the deck displacements corresponding to the wave amplitude input, the displacements being normalised to the standard deviation of the deck displacements. At some point on the displacement-frequency curve, the deck amplitude rises sharply reaching a peak at the wave frequency equalling the fundamental frequency of the offshore platform. This is the resonant frequency; however at this frequency, the amplitude of the platform is prevented from becoming infinitely large by structural damping.

4.2 Offshore Platform Response with an LVA

The model is excited by wave loading, but with an LVA mounted at the deck level. The container radius and liquid height are chosen from Fig. 3.6 such that the natural frequency of the absorber, ω_a, is almost equal to the fundamental frequency, ω_s, of the platform. The programme is run for three different conditions of liquid as shown in Table 4.2. Curve B of Fig. 4.1 shows the deck displacement for

Table 4.1 Structural Data for the Offshore Platform

Height of Platform		366 m
Water Depth		305 m
Base,	External Radius	33.75 m
	Internal Radius	33.60 m
Platform,	External Radius	9.00 m
	Internal Radius	8.90 m
Deck Mass		4180 Mg
Deck Inertia		2432760 Mg m^2
Total Structural Mass		11213 Mg
Modulus of Elasticity		2.039×10^7 kN/m^2
Fundamental Frequency		1.254 rad/s
Viscous Damping,	α	0.0302
	β	0.0043
Hysteretic Damping,	γ	0.015

Run 1 (i.e. with water as the absorber liquid). The vibration of the platform deck at the old resonant frequency (0.2 Hz) is reduced to almost zero, and two new peaks are defined in the vicinity, at 0.185 Hz, and at 0.215 Hz. These two peaks are the new resonant frequencies of the system. The standard deviation of the deck displacement is reduced by 9.4 %. The reduction in the standard deviation (SD) or the root mean square (RMS) value is an indication of the performance of the absorber system. The procedure for Run 2 is the same, but water is replaced with glycerin in the LVA. The effect, as shown in Curve C of Fig. 4.1, is seen to further decrease the vibration around the new resonant peaks (0.185 Hz, 0.215 Hz). The overall effect on the deck displacement is to reduce the standard deviation, σ_x, by 12.6 %. This greater reduction in σ_x is due due to a larger damping ratio in the glycerin than in water. Run 3 is a case where the damping is increased further to ξ_a = 0.05, and the further reduction in the deck displacement response is indicated in Curve D of Fig. 4.1; the reduction in the standard deviation of the deck response is 19 %. The reduction in the standard deviation of the top element strain is 26.2 %.

4.3 Mechanism of Vibration Absorption in a Two-Mass System

The subject of forced vibration of a two-mass model as shown in Fig. 4.2 may be found in a standard text on vibration, and it can be seen that a similar behaviour can be obtained, as in the case of the offshore platform. The two new resonant frequencies depend only on the mass ratio, μ (where μ = m/M), and are determined by the equations

$$(\Omega/\omega_a)^2 = (1 + \mu/2) \pm \sqrt{\mu + \mu^2/4} \qquad (4.1)$$

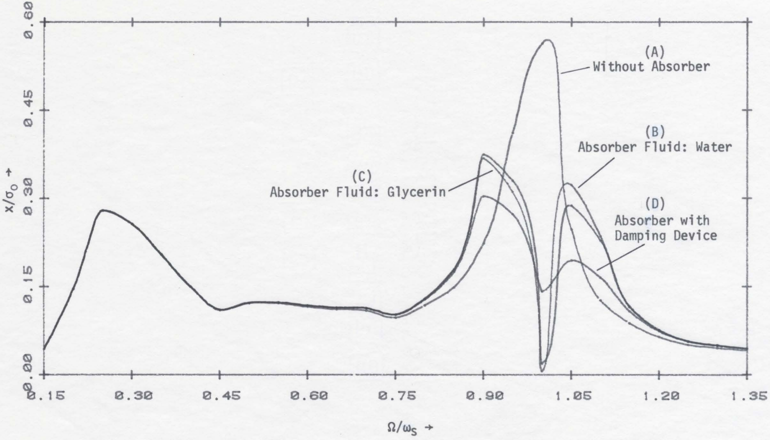

Fig. 4.1 Normalised Deck Displacement Versus Wave Frequency

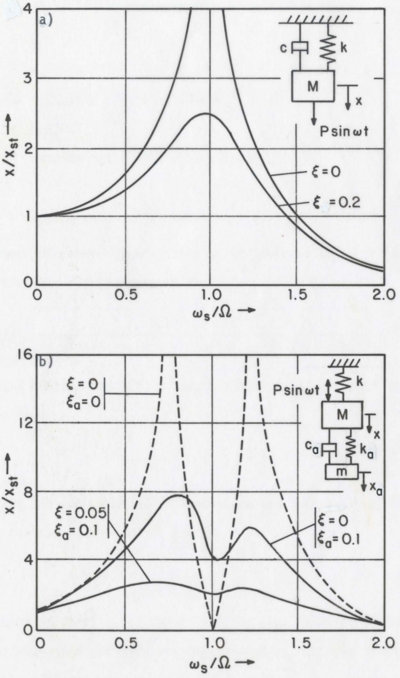

Fig. 4.2 a) Amplitudes of Forced Vibration of a SDOF System for Different Degrees of Damping. b) Amplitudes of Mass M for Various Values of Absorber Damping and Damping of the Main Spring.

where

$\mu = m/M$,

$f = \omega_a/\omega_s$,

ω_s = frequency of the main mass,

$\bar{g} = \Omega/\omega_s$,

ξ = damping ratio of the main spring,

and

ξ_a = damping ratio of the absorber spring.

Den Hartog (18) showed in his study of the dynamic motion of a two-mass model, that the displacement of the main mass is given as

$$\frac{x}{x_{st}} = \sqrt{\frac{(2\xi_a\bar{g})^2 + (\bar{g}^2-f^2)^2}{(2\xi_a\bar{g})^2(\bar{g}^2-1+\mu\bar{g}^2)^2 + (\mu f^2\bar{g}^2 - (\bar{g}^2-1)(\bar{g}^2-f^2))^2}} \tag{4.2}$$

The tuning of the absorber to reduce vibration of the main mass is obtained from

$$f = \frac{1}{1 + \mu} \tag{4.3}$$

Brock (25) and Den Hartog (18) obtained an expression for optimum damping for the same model as follows :

$$\xi_a{}^2 = \frac{3\mu}{8(1 + \mu)^3} \tag{4.4}$$

The results of Refs. 2, 18 and 25 will be used later as guidelines for predicting the optimum absorber parameters required to minimise the offshore platform response to wave loading.

4.4 Comparison of Response Reductions

To compare the performance of the LVA with that of the tuned mass damper of Ref. 2, the original programme of Ref. 2 including a tuned mass damper is used. The inputs to his programme, as shown in Table 4.3, are the equivalent spring-mass-dashpot parameters of the LVA used in 4.2. The comparison of the deck displacement response between the two cases is shown in Fig. 4.3. With the LVA, a larger reduction in the standard deviation of deck response is noted; σ_x for the deck response with LVA is 2 % smaller than that with a tuned mass damper. This small difference is likely to be due to the additional overturning moment caused by the elevations H_1 and H_0, of the masses M_1 and M_0 respectively, increasing the effectiveness of the LVA.

Table 4.2 Damping Ratio of LVA

Run	Cyl. Dimensions R	d	Type	Liquid Properties ν	Density ρ	Damp. Ratio ξ
1	5.6 m	1.6 m	Water	$1\times10^{-6} m^2/s$	$1.00\ Mg/m^3$	0.0001
2	5.6 m	1.6 m	Glycerin	$3\times10^{-3} m^2/s$	$1.25\ Mg/m^3$	0.005
3	5.6 m	1.6 m	Water with Damp Device	$1\times10^{-6} m^2/s$	$1.00\ Mg/m^3$	0.05

Table 4.3 Equivalent Mass Damper Parameters

LVA	Cylinder Radius, R	5.5 m
	Liquid Depth, d	1.6 m
	Kin. Viscosity, ν	$10^{-6}\ m^2/s$
	Liquid Density, ρ	$1\ Mg/m^3$
Mass Damper of Ref. 2	Damper Mass, M_1	97.8 Mg
	Mass, M_0, added to Deck Mass	30.0 Mg
	Damper Frequency, ω_a	0.2003 Hz
	Damping Ratio, ω_a	0.0001

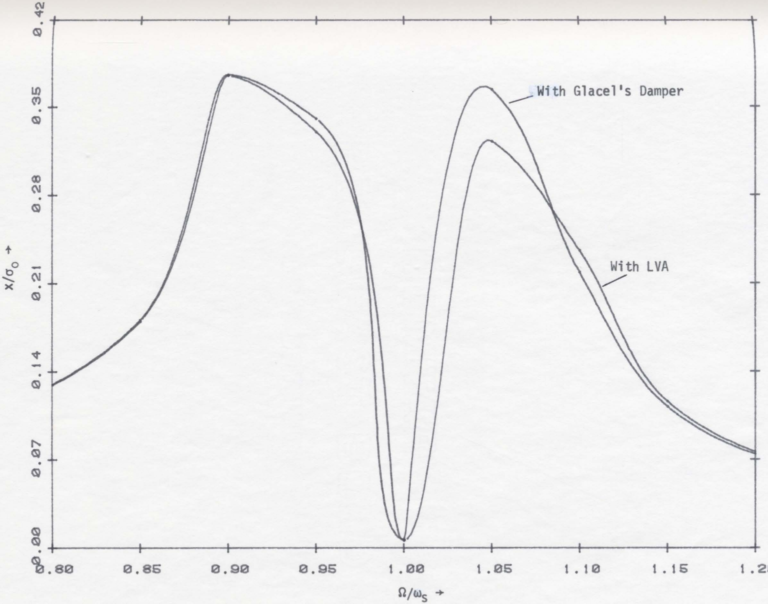

Fig. 4.3 Comparison of the Performance of LVA with Glacel's Damper

CHAPTER 5

OPTIMISATION OF ABSORBER PARAMETERS

5.1 Parameters Affecting Platform Response

The response of the platform with an LVA depends on the parameters μ, f, $\bar{g}$, and ξ_a

where

$$\mu = \frac{\text{Mass of Liquid in Tank}}{\text{Structural Mass of Platform}} = \frac{\rho\pi R^2 d}{M},$$

$$f = \frac{\text{Sloshing Frequency of Absorber}}{\text{Fundamental Frequency of Platform}} = \frac{\omega_a}{\omega_s},$$

$$\bar{g} = \frac{\text{Wave Frequency}}{\text{Fundamental Frequency of Platform}} = \frac{\Omega}{\omega_s},$$

and

$$\xi_a = \text{Damping Ratio of Absorber.}$$

For convenience, μ will be referred to as the mass ratio, f the absorber frequency, $\bar{g}$ the wave frequency, and ω_a the absorber damping ratio. All the four parameters are in dimensionless form.

5.2 Response Reduction with an LVA (without Damping Device)

To find the optimum absorber perfomance, the mass ratio, μ, and the absorber frequency, f, are varied by varying the the tank radius, R, and the depth to radius ratio, d/R.

5.2.1 Liquid Mass Variation

The platform is analysed, with glycerin as the absorber fluid, the absorber frequency, f, held constant at 1.0, and the mass ratio,

μ, varied. In order to vary μ without offsetting the specified value of f, appropriate values of R and d/R are read from Fig. 3.6. The deck diplacement responses obtained from the analyses for three different values of μ are shown in Fig. 5.1; the displacements are normalised to the SD of the deck displacement response without the absorber. The minimum responses for all the three cases occur at the wave frequency, $\bar{g} = f$. Of the three cases, $\mu = 0.013, 0.027$ and 0.053, the smallest SD value of the deck displacement response is obtained for $\mu = 0.013$, for which the two resonant peaks of the displacement-frequency curve are almost at the same level.

The procedure is repeated for more intermediate values of μ. Fig. 5.2 shows the deck displacement-mass ratio curves, each of which corresponds to a particular wave frequency, $\bar{g}_i$. The dominant wave frequencies relevant to the structural model are those in the region around unity as shown in Fig. 5.2 i.e. $\bar{g} = 0.85$ to 1.05. The curves corresponding to these frequencies are indicated by the broken line in Fig. 5.2.

The entire series of simulations are repeated with f = 1.08. Fig. 5.3 presents plots of $\sigma_n - \mu$ curves for the cases f = 1, 1.08, where σ_n is the SD of deck displacement response normalised to the SD of deck displacement response without an LVA. The curves indicate considerable fluctuation of σ_n with varying μ in both cases. This, as will be shown later, is due to the absence of adequate damping in the liquid.

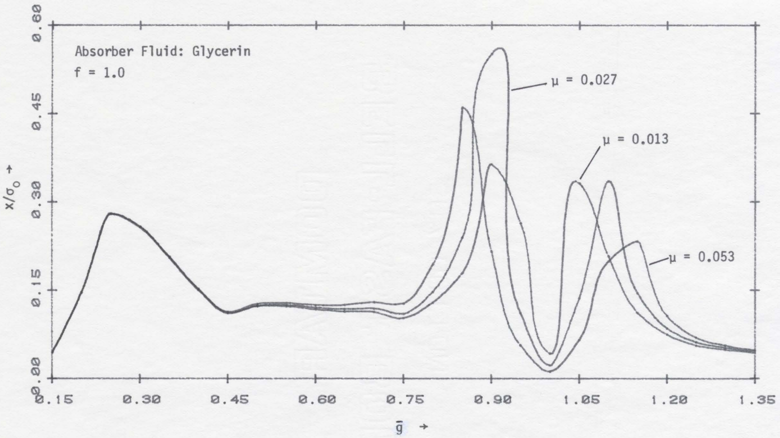

Fig. 5.1 Normalised Deck Displacement Versus Wave Frequency; No Damping Device

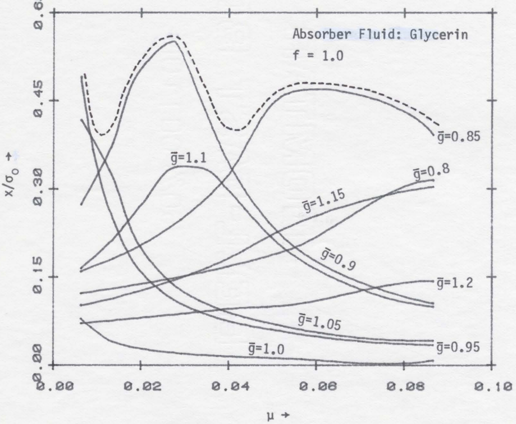

Fig. 5.2 Normalised Deck Displacement Versus Mass Ratio

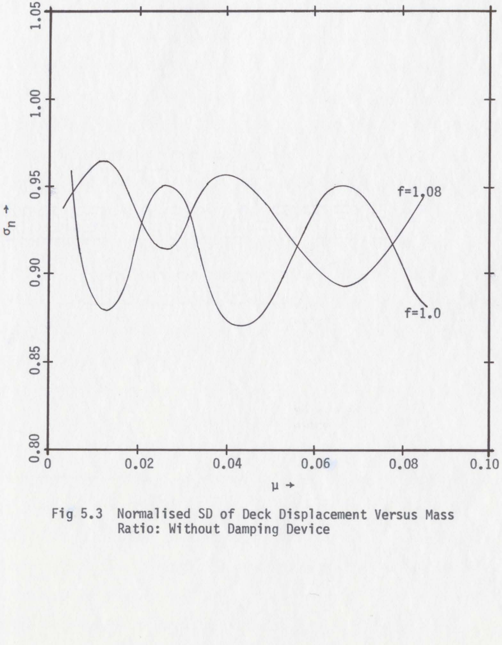

Fig 5.3 Normalised SD of Deck Displacement Versus Mass Ratio: Without Damping Device

5.2.2 Frequency Variation

The absorber frequency, f, is varied, keeping the mass ratio, μ, constant at 0.013, and the fluid viscosity the same as in 5.2.1. The appropriate absorber dimensions are obtained from Fig. 3.6 in order to keep μ constant while varying f. The deck displacement response for three different values of f, 0.8, 1.0 and 1.08, are shown in Fig. 5.4. The resonant peaks exhibit shifts as the absorber frequency, f, is increased or decreased. For $f < 1$, the right resonant peak is the dominant one. As f tends to unity, the right peak falls while the left one rises; at $f \simeq 1.0$, the peaks are at the same level and the minimum SD for the displacement response is obtained. As f is increased further, the left peak continues to rise while the right one falls. Theoretically, as f approaches infinity, the frequency of the absorber will be too large to affect the response of the structure and the right resonant peak disappears while the left peak changes in magnitude, and shifts in position along the wave frequency axis until it is almost similar to the original resonant frequency peak (without absorber).

Fig. 5.5 shows plots similar to Fig. 5.2, but for varying values of f instead of μ. The dominant wave frequencies relevant to the structural model are again shown to be around unity, i.e. $\bar{g} = 0.9$ to 1.05, and the curves corresponding to these frequencies are indicated by the broken line in Fig. 5.5. It can be inferred from the minimum points for the curves (indicated by crosses), that the response of the platform to each particular wave frequency, $\bar{g}_i$, is minimum at the absorber frequency value, $f_i = \bar{g}_i$; this result can be used to optimise the effectiveness of the absorber by shifting the absorber frequency

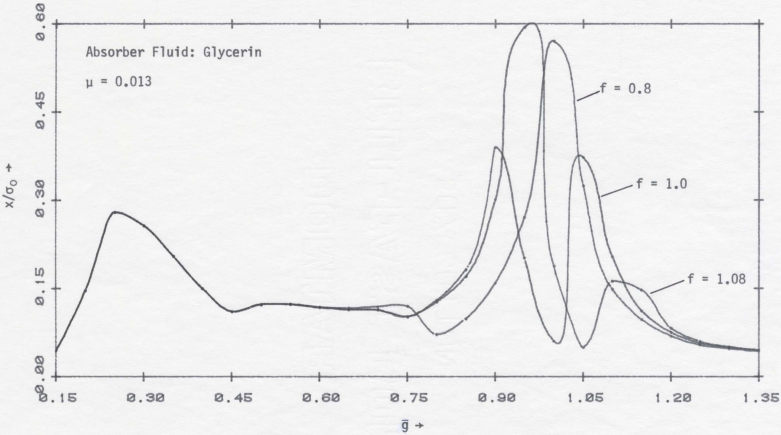

Fig. 5.4 Normalised Deck Displacement Versus Wave Frequency; No Damping Device

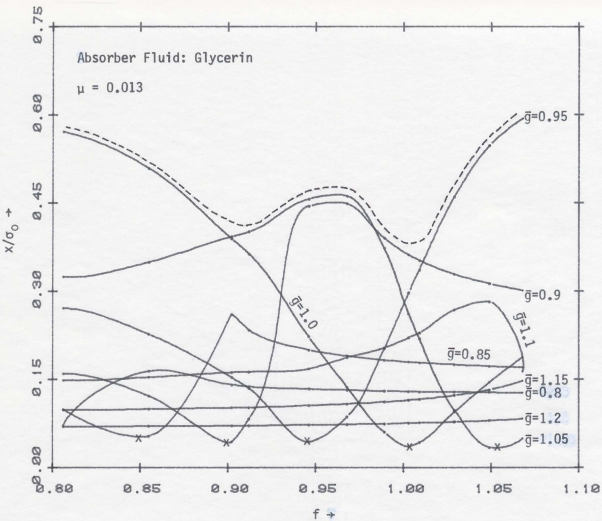

Fig. 5.5 Normalised Deck Displacement Versus Absorber Frequency

into the range of dominant wave frequencies relevant to the platform model, i.e. 0.9 - 1.05. Fig. 5.6 shows the σ_n - f curves for the mass levels μ = 0.013, 0.027. Again, considerable fluctuation of σ_n is noted as the absorber frequency, f, is varied, owing to inadequate damping.

5.3 LVA Application with a Damping Device

To increase energy dissipation in the absorber, the damping ratio is increased from 0.005 to 0.05 by introducing a damping device in the absorber, as discussed in 5.4.

5.3.1 Mass Variation

The mass ratio, μ, is varied, and the absorber frequency, f, kept constant at 0.8, 1.0, and 1.08. Fig. 5.7 shows curves of normalised SD of deck displacement response, σ_n, versus the mass ratio, μ. Each of the curves indicated decreasing σ_n with increasing μ. For f = 1.0 and μ = 0.027, the reduction in the SD value of the deck displacement response is 22 %. As μ is increased, the percentage of reduction in the SD value becomes smaller.

5.3.2 Frequency Tuning

Now, the absorber frequency, f, is varied, keeping the mass ratio, μ, constant at 0.013, 0.027, and 0.04. Plots of σ_n - f curves corresponding to the specified mass ratios are presented in Fig. 5.8. For each case of μ, an optimum absorber frequency, $f_{opt.}$, is obtained. Table 5.1 shows the values of $f_{opt.}$, and the reduction in the SD of the deck displacement response for each case of μ. The optimum frequency values, $f_{opt.}$, as seen from Table 5.1, approach unity as

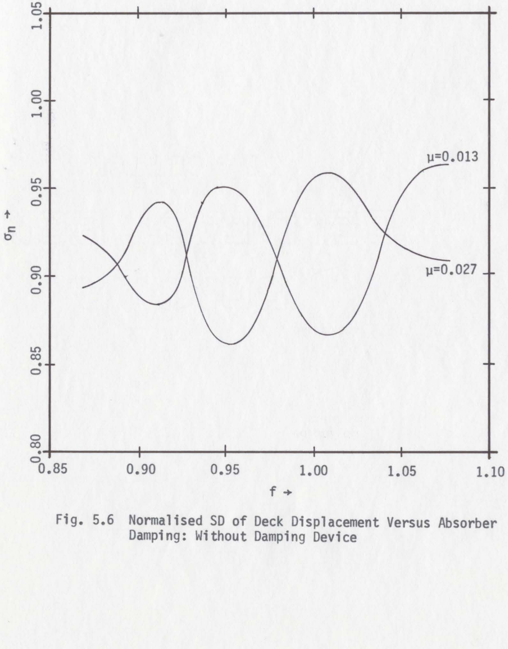

Fig. 5.6 Normalised SD of Deck Displacement Versus Absorber Damping: Without Damping Device

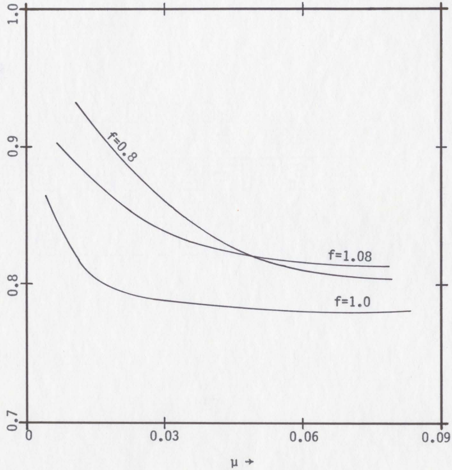

Fig. 5.7 Normalised SD of Deck Displacement Versus Mass Ratio: With Damping Device

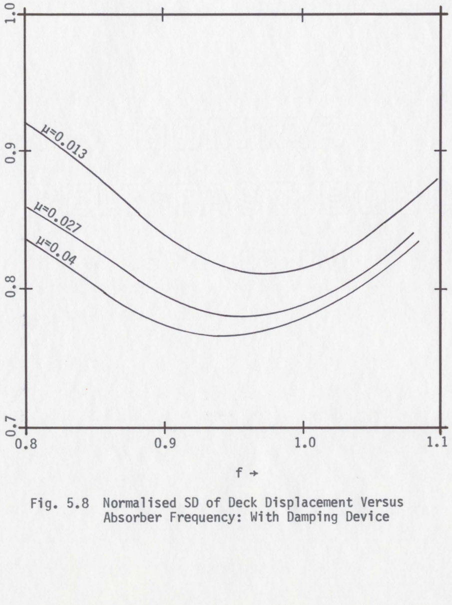

Fig. 5.8 Normalised SD of Deck Displacement Versus Absorber Frequency: With Damping Device

μ tends to zero. This behaviour shows consistency with Eq. 4.3 which was obtained from the two-mass system formulation of Ref. 18. The reduction in the SD value of the top element strain in Case 3 is 32.8 %.

Table 5.1 Optimum Frequencies

Case	Mass Ratio, μ	$f_{opt.}$	Reduction in SD
1	0.013	0.989	18.8 %
2	0.027	0.952	23.5 %
3	0.040	0.940	25.0 %

5.3.3 Optimum Damping

To determine the optimum damping, the damping ratio of the absorber, ξ_a, is varied with f = 1.0 and μ = 0.013. The σ_n - ξ_a curve is presented in Fig. 5.9. As ξ_a increases, σ_n decreases initially, then reaching a minimum at an optimum damping, ξ_a(optimum), and the gradually increases. For f = 1.0 and μ = 0.013, the optimum damping, ξ_a(optimum) = 0.07.

5.4 Damping Devices

Adequate damping of liquid motion may be provided by using fixed baffles attached to the cylinder wall as shown in Fig. 5.10. The baffles may be perforated with the advantage of considerable lightness, and their position along the vertical axis of the cylinder can be controlled. The main effect is the change of first-mode sloshing into a rotary motion. The liquid oscillating in its fundamental mode produces a wave having its maximum amplitude at the cylinder wall.

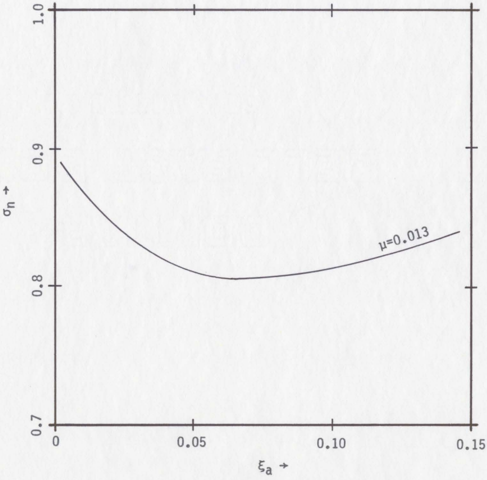

Fig. 5.9 Optimum Absorber Damping

The direction of the liquid motion near the wall is almost vertical and thus normal to the baffle located a small distance, s, beneath the free surface. Energy dissipation results from the baffle resistance on the wave motion, which damps the liquid. The damping of the liquid free surface oscillations in a cylinder by a flat solid ring baffle has been predicted theoretically by Miles (26) in the following form :

$$\xi_a = 2.83\, e^{-4.6s/R} \left(\frac{2w}{R} - \left(\frac{w}{R} \right)^2 \right)^{1.5} \left(\frac{\bar{z}}{R} \right)^{0.5} \tag{5.1}$$

where R, s, w, and $\bar{z}$ are related to the tank geometry as shown in Fig. 5.10. Figs. 5.11 a,b are based on Eq. 5.1 from which ξ_a is obtained with the given parameters R, s, w, and $\bar{z}$. Fig. 5.11 shows that damping decreases exponentially with increasing s/R, indicating that damping is greatest when the baffle is located at the mean free surface level. For the given parameters, w/R = 0.1 and $\bar{z}$/R, with the baffle attached at the mean free surface level, ξ_a = 0.075. For ring baffles, a damping ratio as high as 0.2 to 0.3 is possible. The lowering of sloshing frequencies due to the introduction of a baffle must be taken into account; nevertheless, an increase in damping in the absorber with the use of a ring baffle reduces the structural response, as it increases the rate of energy dissipation in the structural system.

5.5 Frequency Tuning Devices

The natural frequencies of the sloshing liquid in a cylinder can be controlled without adjusting the cylinder geometry and liquid height by using movable devices which are either immersed in the liquid or just cover the liquid surface. Siekmann and Chang (27) made

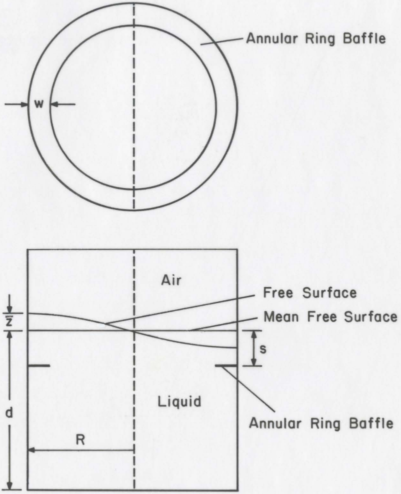

Fig. 5.10 Damping Device

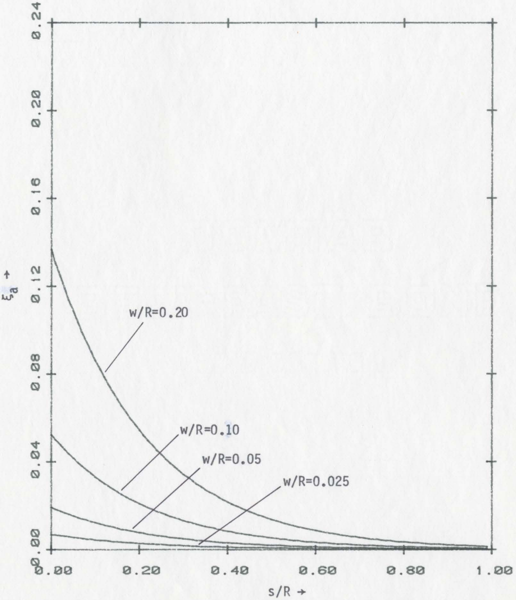

Fig. 5.11a Damping Factor of LVA as a Function of Baffle Depth for z/R = 0.05

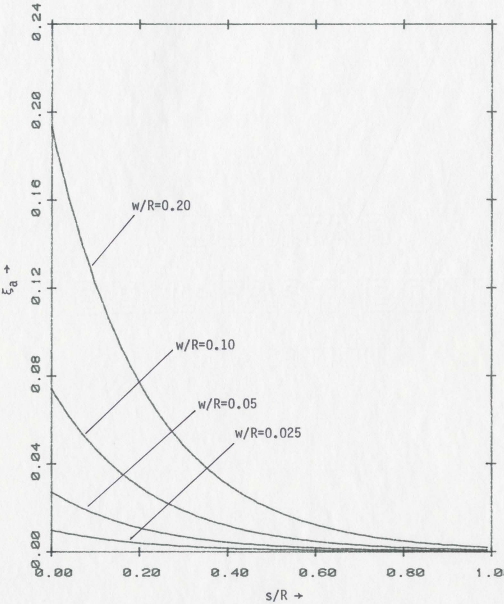

Fig. 5.11b Damping Factor of LVA as a Function of Baffle Depth for z/R = 0.1

a theoretical study on the control of natural frequencies of a sloshing liquid in an upright cylindrical container. The liquid domain is divided into two regions, ϕ_1 and ϕ_2, by means of an elastic mat which is either a membrane or a plate as shown in Fig. 5.12. The mat is attached to the tank wall at a height h, such that the edge of the mat, though movable, will remain at this height during sloshing. For the case where the membrane covers the liquid surface, the fundamental frequency is given by Ref. 27 as

$$\omega^2 = \frac{\rho g k + \tau k^3}{\rho \cosh(kd) + \rho_m k \sinh(kd)} \sinh(kd) \qquad (5.2)$$

where

ρ = density of fluid,

g = gravitational acceleration,

τ = tensile force per unit length in membrane,

ρ_m = mass per unit area of membrane,

k = constant, $k = 1.84/R$,

and

R = cylinder radius.

For the case of an elastic plate covering the free surface,

$$= \frac{Dk^5 + \rho k g}{\rho_p \bar{t} k \sinh(kd) + \rho \cosh(kd)} \sinh(kd) \qquad (5.3)$$

where

D = flexural plate rigidity, $D = \dfrac{E\bar{t}^3}{12(1-\nu^2)}$,

E = Young's modulus,

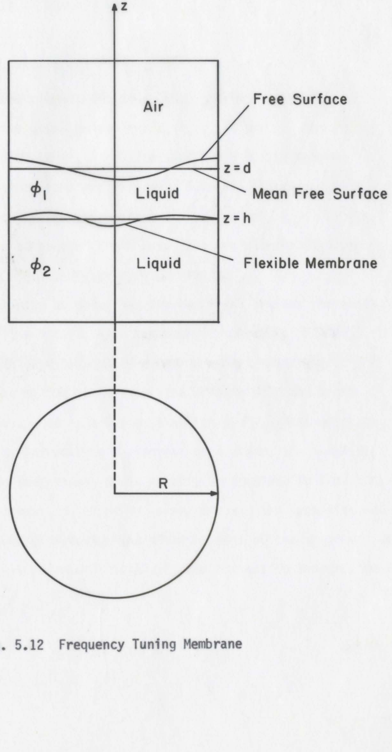

Fig. 5.12 Frequency Tuning Membrane

ν = Poisson's ratio,

ρ_p = density of plate material,

and

$\bar{t}$ = plate thickness.

Figs. 5.13 a,b, and c are based on Eq. 5.2, giving the sloshing frequencies for the given parameters ρ, τ, ρ_m, d and R. Given the parameters, ρ = 1000 kg/m , d = 1.3 m, and R = 6 m, the natural sloshing frequency as obtained from Fig. 3.6 is 1.08 rad/s. With the application of an elastic membrane (τ = 30 kN/m , ρ_m = 20 kg/m) covering the free surface of the liquid, the new sloshing frequency, as obtained from Fig. 5.13c, is ω_a = 1.2 rad/s.

It is of interest to note that the membrane, besides increasing the frequency of the liquid, also increases the damping in the liquid motion. In this respect, the membrane may prove to be effective in reducing the response of the structure if the right damping and frequency can be achieved simultaneously. Another point to note is that by introducing a membrane or a plate, the sloshing force tends to be suppressed, and a penalty is involved in that part of the convective mass, M_1, that is converted into the impulsive mass. This has the effect of reducing the effectiveness of the absorber (as the oscillating liquid mass is smaller), and increasing the deck mass.

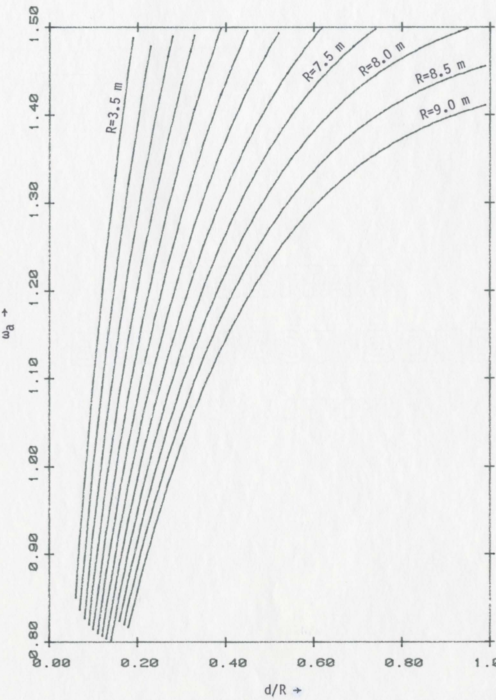

Fig. 5.13a Change of Sloshing Frequency Using an Elastic Membrane with τ = 10 kN/m

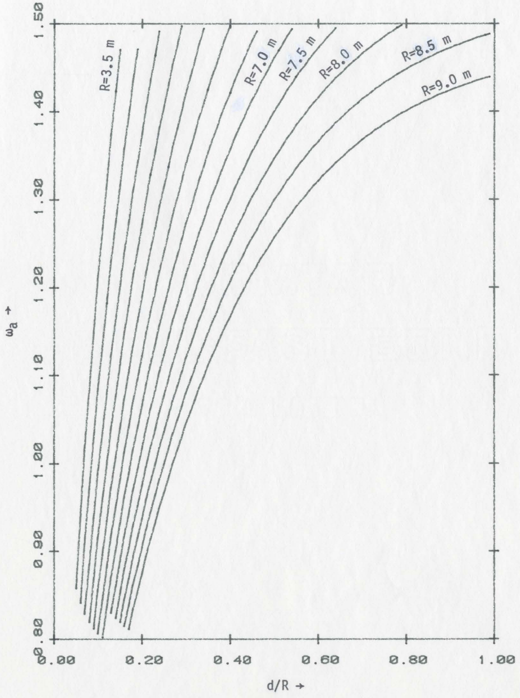

Fig. 5.13b Change of Sloshing Frequency Using an Elastic Membrane with τ = 20 kN/m

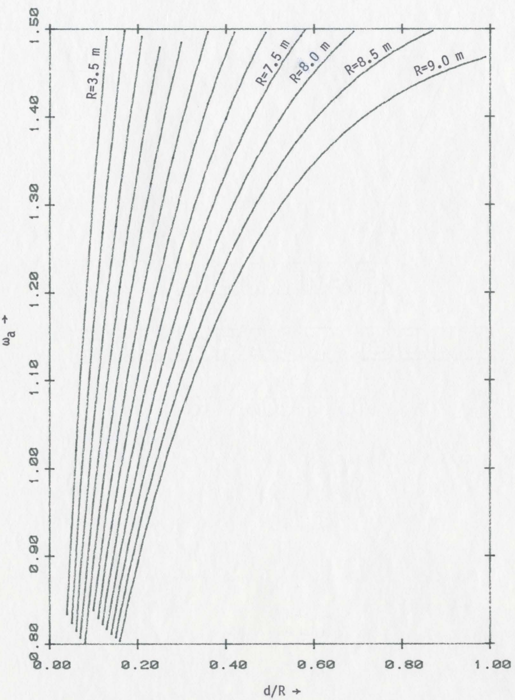

Fig. 5.13c Change of Sloshing Frequency Using an Elastic Membrane with τ = 30 kN/m

CHAPTER 6

CONCLUSIONS AND DISCUSSION

6.1 Conclusion

6.1.1 Absorber without Damping Device

i) When the LVA is mounted on the platform model, the platform response was reduced. The response reduction is dependent on the liquid mass and frequency, and the damping ratio of the liquid motion (in another sense, dependent on the cylinder radius, the depth to radius ratio, and the liquid viscosity and density). The reduction of the standard deviation of the deck displacement response for a 5.5 m - radius cylinder with glycerin filled to depth 1.6 m is 12.6 %.

ii) The platform response fluctuates in both cases - varying liquid mass and sloshing frequency; hence the optimum mass and freque-cy for minimum response cannot be defined.

6.1.2 Absorber with Damping Device

i) When the absorber fluid is damped with a damping device, the response reduction is significantly greater. For f (absorber frequency) = 1.0, and μ (mass ratio) = 0.013, the optimum damping, ξ_a(optimum) = 0.07.

ii) The platform response reduces with an increase in liquid mass, but as the liquid mass is increased further in the subsequent simulations, the percentage of response reduction is smaller.

iii) An optimum absorber frequency can be obtained for each value of liquid mass. For the mass ratio, μ = 0.04, the optimum absorber frequency, f = 0.94; the corresponding reduction in the standard deviation of the deck displacement response is 25 %.

iv) The reduction in the standard deviation in the top element strain for $\mu = 0.04$, f = 0.94, and $\xi_a = 0.05$, is 32.8 %. The reduction in the strain response increases the fatigue life of the structure.

6.2 Discussion

The standard deviation (SD or σ) of the deck displacement is indicative of the overall structural response, and the SD of the element strain indicates the stress response of the member. The reduction in the SD of member stresses reduces the probability of exceeding the ultimate stress limit of the member. Moreover, if fatigue is the mode of failure, the number of cycles to failure is increased when the SD of member stress levels is reduced (28, 29). The reduction of the deck acceleration is important from the consideration of human comfort and instrumentation.

The advantages of the LVA over the tuned mass damper are :

i) It is less costly in installation and maintenance,

ii) As the LVA is cylindrical, it can function in any horizontal direction,

iii) The horizontal liquid motion is restricted by the cylinder wall, hence less platform space is required for the absorber operation

and

iv) The liquid mass can be easily controlled by pumping operations to and from the base of the platform.

PART TWO

SEISMIC RESPONSE OF ELEVATED LIQUID STORAGE TANKS

CHAPTER 7

INTRODUCTION

Investigations of the seismic behaviour of elevated liquid storage structures have been motivated by numerous events of earthquake damage and destruction of elevated water tanks in places of high seismicity. Housner (3) proposed a method of determining the hydrodynamic pressures in a rigid fluid container subject to horizontal accelerations. This enabled the representation of the elevated liquid storage tank by a two-mass system, a method commonly used in succeeding investigations on the seismic response analysis of elevated water tanks. Although the two-mass system is a reasonable representation for the elevated water tank, study of the seismic behaviour appears to be adequate only for the supporting structure. A report by Hill and Biggs (30) indicated that although most of the earthquake damage to water towers occurred in the supporting structure, some were due to the structural inadequacy of the storage tank itself. Veletsos and Yang (31) reported that the hydrodynamic effects in flexible tanks may be larger than those in rigid tanks of the same dimensions. The current seismic design coefficients for water storage towers are of a significantly higher order than those for buildings. This possible conservatism may be a reflection of uncertainties (e.g. those reported by Refs. 30 and 31) in the stress behaviour induced by hydrodynamic effects.

The majority of elevated water tanks have been in the 600 m^3 class or smaller. More recently, tank sizes up to 12000 m^3 (Fig. 7.1e) have been constructed, most of them in steel or concrete. The supporting structure may consist of a frame (Fig. 7.1a), a multicolumn assembly (Fig. 7.1b), or an axisymmetric pedestal (Figs. 7.1c,d,e). As many elevated water tanks of today are much larger in dimensions than those previously constructed, more sophisticated method of analysis are required to determine their seismic behaviour. The considerable need for predicting the response of the larger liquid storage tower structures, incorporating detailed shell behaviour of the tank, has initiated the studies described in this report. The work is restricted to the formulation of a procedure for seismic analysis of axisymmetric water towers, an extension of the work by Balendra and Nash (32) on the seismic response analysis of ground-supported liquid storage tanks. Much of the information is presented without proof, and mathematical details may be followed up through the quoted references. A study of the soil-structure interaction effect is beyond the scope of this work.

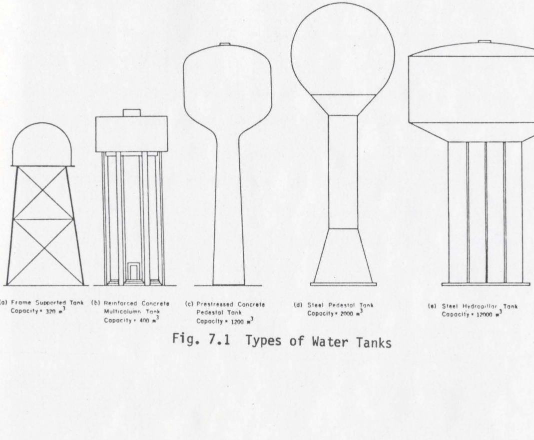

Fig. 7.1 Types of Water Tanks

CHAPTER 8

LITERATURE REVIEW

8.1 Dynamic Analysis of Ground-Supported Cylindrical Tanks

Early studies of the forced vibration of contained liquids go back to 1950; significant and theoretical investigations are those of Jacobsen (33), and Jacobsen and Ayre (34) which dealt with the seismic behaviour of rigid cylindrical tanks. Ref. 33 calculated the forces and moments induced by the fluid inside a cylindrical tank subjected to horizontal acceleration. Ref. 34 conducted experiments on liquid-filled cylindrical tanks, with damped harmonic excitation of tank bases. The work was followed by Housner's (3) formulation of simplified expressions for obtaining the hydrodynamic pressures developed in rigid ground-supported tanks, subjected to horizontal acceleration. Satisfactory agreement between the behaviour of petroleum storage tanks in the 1964 Alaskan earthquake and the predictions based on the work of Ref. 3, has been demonstrated by Shepherd (35). During the past decade, there has been a rapid development in the subject related to the sloshing behaviour of liquids in fuel tanks of liquid propellant rockets. In the field of aerospace technology, Lindholm, Kana and Abramson (36), Chu (37), Kana and Chu (38), DiMaggio and Bleich (39), and Fung, Sechler and Kaplan (40) made valuable contributions to the response analysis of pressurized cylinders containing liquids. Luk (41) presented a development of a finite element model, and some numerical examples for liquid sloshing problems involving both rigid and axisymmetric containers. Edwards (42) investigated coupled interaction between the elastic walls of a cylindrical tank and the contained liquid, and simulated the liquid-filled tank with ground motion by numerical integration. Bauer and Siekmann (43) analysed the general case of hydroelastic coupled oscillations of a partially-filled liquid container with a flexible bottom and an elastic side wall.

More recently, Wu, Mouzakis,Nash and Colonell (44), Shaaban and Nash (45), and Balendra and Nash (32) made significant contributions to the advancement on the seismic analysis of ground-supported liquid-filled cylindrical tanks. Ref. 44 presented an analytical formulation and developed a computer programme for determination of natural frequencies of free vibration of an elastic circular shell partially filled with liquid. Ref. 45 developed a finite element computer programme for the time-history analysis of seismic response of ground supported liquid-filled tank, while Ref. 32 expanded the work to include an axisymmetric dome top. Recent experimental investigations by Clough and Clough (46) on the seismic behaviour of ground-supported liquid-filled cylindrical tanks have indicated significant cross-sectional distortion of elastic tanks caused by uplifting of the base, and geometric imperfections of the side wall, which had not been included in theoretical predictions.

8.2 Seismic Response of Elevated Water Tanks

Literature related to the dynamic behaviour of elevated water tanks dates back to as early as 1936, when Carder (47) tested steel water tanks, by a series of pull-back tests on the supporting towers, to study the effects of the foundation conditions and tower motion in seismic events. Extensive model studies were undertaken by Ruge (48) with the object of deriving data useful for the seismic design of water tanks. Many of the later investigations used the method of determining hydrodynamic pressures proposed by Ref. 3. Both Cloud (49) and Blume (50) have reported reasonable correlation between the observed behaviour of water tanks and the vibrational parameters obtained from the method of Ref. 3. Chandrasekaran and Krishna (51) have reported an analytical investigation of the seismic behaviour of reinforced concrete water towers. Simplification of the elevated tank with a two-mass idealization have also been used in the work of Sonobe and Nishikawa (52), Ifrim and Bratu (53), Garcia (54), and Shepherd (55). Ref. 55 studied the free vibrations of an axisymmetric prestressed concrete elevated water tank, and carried out a simple pull-back test to substantiate the validity of the theoretical model.

CHAPTER 9

THEORY USED

9.1 Shell Mass and Stiffness Matrices

The mass and stiffness matrices, $\underline{M}_s$ and $\underline{K}_s$, for the axisymmetric shell structure are generated by using the finite element computer code SAMMSOR-II (56). The programme idealises the shell of revolution by curved ring elements, developed by Stricklin, Navaratna and Pian (57). The displacements of an element in the meridional, circumferential, and normal directions, denoted by u, v, and w respectively, are represented by a Fourier representation in the circumferential direction as follows :

$$\sum_m u = u_m(z,t) \cos m\theta \, , \qquad (9.1a)$$

$$\sum_m v = v_m(z,t) \sin m\theta \, , \qquad (9.1b)$$

and

$$\sum_m w = w_m(z,t) \cos m\theta \, , \qquad (9.1c)$$

where u_m, v_m, and w_m are the generalised displacements for the m th circumferential harmonic.

9.2 Equations of Motion of Liquid

Fig. 9.1 shows the coordinate system (r,θ, z) adopted in defining the equations governing the liquid motion. For an inviscid, incompressible liquid, the governing equations of motion are the Laplace equation

$$\nabla^2 p(r,\theta,z) = 0 \, , \qquad (9.2)$$

and the Bernoulli Equation

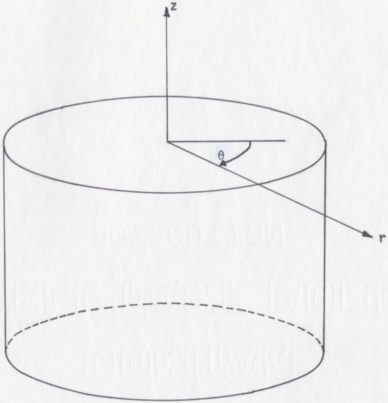

Fig. 9.1 Coordinate System

$$\frac{\partial \phi}{\partial t} + \frac{p}{\rho_f} + gz = 0 \tag{9.3}$$

where $\phi(r,\theta,z)$ is the velocity potential, p the liquid pressure, ρ_f the liquid density, and g the gravitational acceleration.

9.3 Boundary Conditions

At the free surface, the boundary equation may be expressed as

$$\left.\frac{\partial^2 \phi}{\partial t^2}\right|_{z=0} + g \left.\frac{\partial \phi}{\partial z}\right|_{z=0} = 0 \tag{9.4}$$

At the elastic cylindrical tank wall, the boundary condition expressing the liquid solid-interaction is given as

$$\left.\frac{\partial \phi}{\partial r}\right|_{r=R} = \left.\frac{\partial w}{\partial t}\right|_{r=R} \tag{9.5}$$

At the rigid tank bottom, the boundary condition is written as

$$\left.\frac{\partial \phi}{\partial z}\right|_{z=-H} = 0 \tag{9.6}$$

9.4 Coupled Liquid-Tank Interaction

The variational functional for the liquid is given as

$$I = \int_{t_1}^{t_2} (T - \Pi - W) \, dt \tag{9.7}$$

where T, Π, and W are the kinetic and potential energies, and the the work done on the liquid respectively. Hsiung and Weingarten (58) obtained T by integration over the liquid volume V, Π by integration over the free surface F, and W by integration over the liquid-tank interface Σ, as follows:

$$T = \frac{\rho_f}{2}\int_V \nabla\phi \cdot \nabla\phi \, dV , \qquad (9.8a)$$

$$\Pi = \frac{1}{2}\int_F \xi(\rho_f \, g \, \xi) \, dS , \qquad (9.8b)$$

and

$$W = \int_\Sigma \rho_f \left(\frac{\partial w}{\partial t} \right)\phi \, dS \qquad (9.8c)$$

where ρ_f is the liquid density, ξ the liquid elevation from the mean free surface level, and $\nabla\phi$ the velocity vector $\overline{v}$ given by

$$\overline{v} = \text{grad } \phi \qquad (9.9)$$

It has been shown by Ref. 58 that the functional involving the governing equations 9.2 and 9.3, together with the boundary equations 9.4, 9.5 and 9.6, can be expressed in the form

$$I = \frac{1}{2}\int_V \nabla p \cdot \nabla p \, dV - \frac{g}{2}\int_F \left(\frac{\partial p}{\partial t} \right)^2 dS - \rho_f \int_\Sigma p \, \frac{\partial^2 w}{\partial t^2} \, dS \qquad (9.10)$$

Ref. 32 discretised the liquid in the cylindrical tank into annular elements of rectangular cross-section, and expressed Eq. 9.10 in terms of element nodal pressure vector, $\underline{P}$, and the shell nodal displacement vector, $\underline{U}$, giving the variational functional in matrix form as follows:

$$I = \frac{1}{2}\underline{P}^T \underline{K}_f \underline{P} - \frac{1}{2}\dot{\underline{P}}^T \underline{M}_f \dot{\underline{P}} - \rho_f \underline{P} \, \underline{S} \, \ddot{\underline{U}} \qquad (9.11)$$

where $\underline{K}_f$, $\underline{M}_f$, and $\underline{S}$ are the liquid stiffness, liquid mass, and coupling force matrices respectively. Minimizing the variational functional by the Euler-Lagrange procedure gives the following matrix equation

$$\underline{K}_f \underline{P} + \underline{M}_f \ddot{\underline{P}} - \rho_f \underline{S} \, \ddot{\underline{U}} = 0 \qquad (9.12)$$

The equations for the dynamic fluid pressure on the shell is given by (59):

$$\underline{M}_s \ddot{\underline{U}} + \underline{K}_s \underline{U} + \underline{S}^T \underline{P} = 0 \qquad (9.13)$$

By using Eqs. 9.12 and 9.13, and neglecting the free surface pressure of the liquid, the equations of motion representing the free vibration of the coupled liquid-tank system were obtained by Ref. 32 as follows:

$$[\, \underline{M}_s + \underline{A} \,] \ddot{\underline{U}} + \underline{K}_s \underline{U} = 0 \qquad (9.14)$$

in which $[\, \underline{M}_s + \underline{A} \,]$ is the modified mass matrix accounting for the hydrodynamic effect of the liquid. The matrix, $\underline{A}$, generated by the computer code, FLUID, developed by Ref. 32 is given by :

$$\underline{A} = \underline{S}^T \underline{K}_f \underline{S} \qquad (9.15)$$

9.5 Response Analysis of an Elevated Water Tank

The tower in Fig. 7.1c is the example problem for the analysis. The mass and stiffness matrices of the elevated liquid-filled tank are generated based on the theory outlined above, while the mass and stiffness matrices of the outer shell of the supporting pedestal are generated separately by the computer code of Ref. 56. The inner tube, carrying the piping connections, and enclosed by the spiral staircase, contributes a negligible amount to the stiffness of the supporting structure, but in view of its concentricity with the outer shell, its stiffness can be added to the stiffness of the outer shell to obtain the combined stiffness of the supporting structure. The sloshing due to the liquid part filling the conical base of the tank is assumed negligible, and the water in this region is treated as a solid mass.

After assembling the matrices of the tank and supporting structure to form the overall matrices $\underline{M}$ and $\underline{K}$, and imposing the boundary conditions at the foundation (fixed in this case), the frequencies, ω, and the mode shapes, ϕ, of the structure are obtained first by matrix decomposition using Choleski's method, and then solved by a standard eigenvalue subroutine.

The Rayleigh damping matrix is given by :

$$\underline{C} = a_0 \underline{M} + a_1 \underline{K}, \tag{9.16}$$

where

$$\begin{Bmatrix} a_0 \\ a_1 \end{Bmatrix} = 2.0 \begin{bmatrix} 1/\omega_1 & \omega_1 \\ 1/\omega_2 & \omega_2 \end{bmatrix} \begin{Bmatrix} \xi_1 \\ \xi_2 \end{Bmatrix}$$

The partitioned matrix equation of motion may be written as

$$\begin{bmatrix} \underline{M} & \underline{M}_c \\ \underline{M}_c^T & \underline{M}_g \end{bmatrix} \begin{Bmatrix} \ddot{\underline{U}}_t \\ \ddot{\underline{U}}_g \end{Bmatrix} + \begin{bmatrix} \underline{C} & \underline{C}_c \\ \underline{C}_c^T & \underline{C}_g \end{bmatrix} \begin{Bmatrix} \dot{\underline{U}}_t \\ \dot{\underline{U}}_g \end{Bmatrix} + \begin{bmatrix} \underline{K} & \underline{K}_c \\ \underline{K}_c^T & \underline{K}_g \end{bmatrix} \begin{Bmatrix} \underline{U}_t \\ \underline{U}_g \end{Bmatrix} = \begin{Bmatrix} 0 \\ \underline{F}_g \end{Bmatrix}, \tag{9.17}$$

in which the lower segment of Eq. 9.17 pertains to the base nodal displacements, and the upper segment to the non-base nodal displacements. $\underline{M}_c$, $\underline{C}_c$, and $\underline{K}_c$ are the coupling effects between the base and non-base nodes. The total displacements, $\underline{U}_t$, of the off-base nodes can be expressed as the sum of the pseudostatic component, $\underline{U}_s$, and the dynamic component, $\underline{U}$, as follows :

$$\underline{U}_t = \underline{U}_s + \underline{U} \tag{9.18}$$

The vector, $\underline{U}_s$, is considered to be developed through rigid body displacements resulting from $\underline{U}_g$, and the relationship is given by

$$\underline{K}_c \underline{U}_g + \underline{K} \underline{U}_s = 0 \tag{9.19}$$

This can be rewritten as

$$\underline{U}_s = \underline{R} \underline{U}_g, \tag{9.20}$$

in which $\underline{R} = -\underline{K}^{-1}\underline{K}_c$.

The equations for the off-base elements in Eq. 9.17 can be written as

$$\underline{M}\,\ddot{\underline{U}} + \underline{C}\,\dot{\underline{U}} + \underline{K}\,\underline{U} = -[\underline{M}\,\underline{R} + \underline{M}_c]\ddot{\underline{U}}_g - [\underline{C}\,\underline{R} + \underline{C}_c]\dot{\underline{U}}_g \qquad (9.21)$$

The terms on the right-hand side are the effective earthquake forces, and if the velocity dependent term, $[\underline{C}\,\underline{R} + \underline{C}_c]\dot{\underline{U}}_g$, is neglected*, Eq. 9.21 would reduce to

$$\underline{M}\,\ddot{\underline{U}} + \underline{C}\,\dot{\underline{U}} + \underline{K}\,\underline{U} = -[\underline{M}\,\underline{R} + \underline{M}_c]\ddot{\underline{U}} = \underline{P}_{eff} \qquad (9.22)$$

where $\underline{P}_{eff}$ is the effective force vector. Eq. 9.22 can be decoupled by substituting $\underline{U} = \underline{\phi}\,\underline{Y}$, and pre-multiplying the result by $\underline{\phi}^T$; the individual equation for the ith mode is obtained as follows :

$$\ddot{Y}_i + 2\,\xi_i\,\omega_i\,\dot{Y}_i + \omega_i^2\,Y_i = P_i/M_i \qquad (9.23)$$

where $P_i = \underline{\phi}_i^T\,\underline{P}_{eff}$, and $\underline{M}_i = \underline{\phi}_i^T\,\underline{M}\,\underline{\phi}_i$.

Y(t) for the mode number specified is found by Duhamel integration, from which $\underline{U}(t)$ is obtained. By omitting the terms $[\underline{C}_g + \underline{C}_c\,\underline{R}]$ and $[\underline{K}_g + \underline{K}_c\,\underline{R}]$ from Eq. 9.17, the reactions at the foundations can be given as

$$\underline{F}_g = [\underline{M}_g + \underline{M}_c\,\underline{R}]\ddot{\underline{U}}_g + \underline{M}_c\,\ddot{\underline{U}} + \underline{C}_c\,\dot{\underline{U}} + \underline{K}_c\,\underline{U} \qquad (9.24)$$

Consequently, the stress resultants, N_s, N_θ and $N_{s\theta}$, and the stress couples, M_s, M_θ and $M_{s\theta}$, are computed at all the nodes for the specified circumferential angles θ. The programme of Ref. 32 is modified to include damping, and generalise its applicability to elevated liquid storage tanks.

* The damping contribution to the effective earthquake forces is small, and is usually neglected (60).

CHAPTER 10

NUMERICAL ANALYSIS

10.1 Structural Data

The dimensions and properties of the elevated tank are shown in Fig. 10.1. The number of elements employed is 35 as shown in Fig. 10.2, and the first eight modes are shown in the main response analysis.

10.2 Criterion for Selecting Damping Ratio

The damping ratio for liquid motion is relatively small, ranging from 0.0001 to 0.005, while the structural damping ratio is much larger in value as shown in Table 10.1.

Table 10.1 Damping Ratio of an Empty Elevated Tank

Type of Structural Material	Damping Ratio, ξ
Steel	0.005 to 0.02
Concrete	0.05 to 0.07
Masonry	0.15 to 0.40

At present, there is no definite rule on which to base the computation of the damping ratios for the whole elevated tank system containing liquid . The damping ratio for the overall system depends om the amount of influence from the liquid motion, as well as the motion of the supporting structure. When the tank is either empty or completely full, no sloshing is involved, and the first and second mode damping ratios, ξ_1 and ξ_2, are both chosen as 0.05 for the structure to

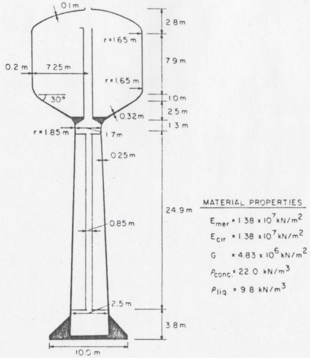

Fig. 10.1 Dimensions and Material Properties

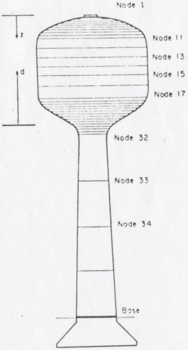

Fig. 10.2 Node Numbering

be analysed. When partially filled with water, the first mode involves sloshing almost entirely, whereas the second mode essentially involves the motion of the supporting structure. Hence, it seems reasonable to use $\xi_1 = 0.001$ and $\xi_2 = 0.05$ for partially filled elevated tanks. From the damping ratios chosen, the appropriate damping coefficients, a_0 and a_1 can be determined.

10.3 Load Input and Simulation

The ground acceleration depends on the level of seismic resistance sought. For the present example, the digitised S69E ground acceleration of the 1952 TAFT earthquake with a 0.2g peak amplitude is provided as the input to the programme. The first circumferential mode of the structure is excited, giving a series of displacement-time responses. The stress resultants and couples at the midpoint of each element, and the foundation reactions are also obtained. The procedure is repeated for different cases of liquid depths. The analysis is also carried out for an empty elevated tank, with weight equal to the weight of the liquid-filled tank to simulate the no-sloshing case. The four different cases considered in the analysis of the tower are shown in Table 10.2.

Table 10.2 Cases of Analysis

Case	Water Depth, d	ξ_1	ξ_2	Liquid Condition
I	7.25 m	0.001	0.05	Include Sloshing
II	11.00 m	0.001	0.05	Include Sloshing
III	11.00 m	0.05	0.05	Include Sloshing
IV	11.00 m	0.05	0.05	Sloshing Suppressed

10.4 Results and Discussion

The predicted free vibration frequencies, as shown in Table 10.3, decreased significantly as the water depth is increased. This is due to the effect of increasing the mass near the top of the structure as the water depth is increased. It is also noted that the case including sloshing (III) gives higher frequencies than the no-sloshing case (IV); this may be due to the considerably larger 'impulsive' mass (referred to in 3.7 as the liquid mass which moves in unison with the structure) in the latter.

Displacement plots, Figs. 10.4 a,b,c and d, show that the maximum radial displacements for all the four cases occur at time t = 3.4 s. The differences between the responses for the cases considered are small as the supporting structure is relatively stiff. The displacement responses obtained for Case II ($\xi_1 = 0.001$, $\xi_2 = 0.05$) are larger than those for Case III ($\xi_1 = 0.05$, $\xi_2 = 0.05$) due to the larger first mode damping in the latter. This suggests that larger dynamic response of the water tank can result from possible influence on the first mode motion by the sloshing of liquid, which introduces smaller damping ratios.

The maximum values of the foundation are also obtained at t = 3.4 s and shown in Table 10.4. From Table 10.4, the results show that for most instances, Case III (sloshing included) gives larger responses than for Case IV (sloshing not included) at the tank wall, and smaller responses at the supporting structure, indicating a possible amplification of the stress response in the tank region caused by liquid sloshing.

Case I gives larger displacements than Case II at the tank wall,

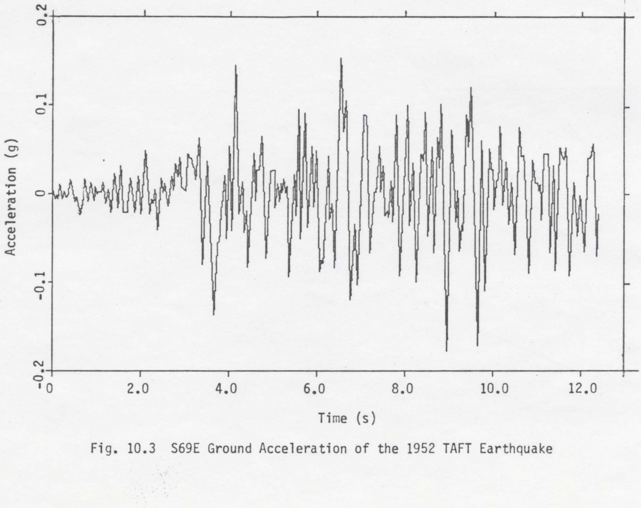

Fig. 10.3 S69E Ground Acceleration of the 1952 TAFT Earthquake

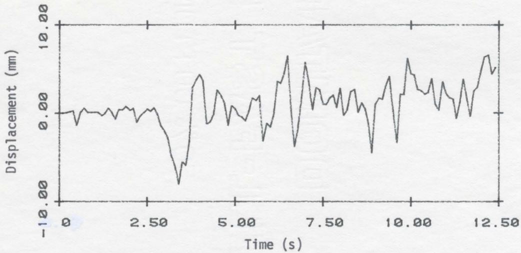

Fig. 10.4a Radial Displacement Response of Node 15 for Case I: Water Depth of 7.25 m, $\xi_1 = 0.001$, $\xi_2 = 0.05$.

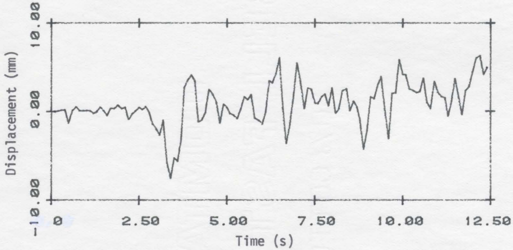

Fig. 10.4b Radial Displacement Response of Node 15 for Case II: Water Depth of 11.0 m, $\xi_1 = 0.001$, $\xi_2 = 0.05$.

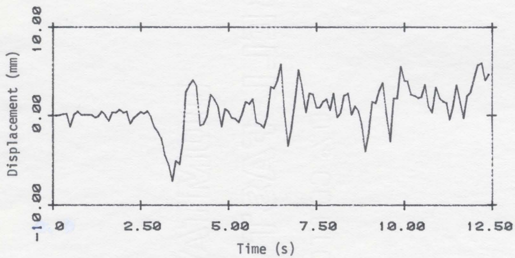

Fig. 10.4c Radial Displacement Response of Node 15 for Case III: Water Depth of 11.0 m, $\xi_1 = 0.05$, $\xi_2 = 0.05$.

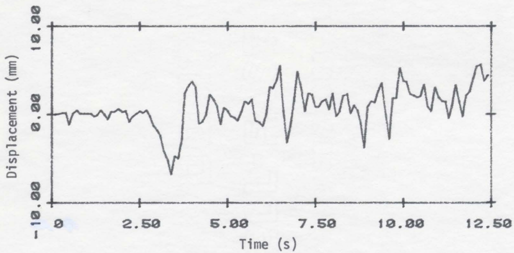

Fig. 10.4d Radial Displacement Response of Node 15 for Case IV: Water Depth of 11.0 m, $\xi_1 = 0.05$, $\xi_2 = 0.05$, Sloshing Suppressed.

suggesting that the larger liquid volume does not necessarily cause greater response to ground excitation.

The stresses obtained at the tank wall are at their maximum at time t = 12.1 s. Table 10.5 presents the stress resultants at the midpoints of Elements 15 and 17 at t = 12.1 s for the cases considered. The results show that the base of the tower has the largest force resultants at any instant. As far as the tank wall is concerned, the bottom of the storage tank is the most stressed region. The total axial moment at the midpoints of Elements 17 (near tank bottom) and and 35 (tower base) can be computed by multiplying M_s (axial moment per unit length) at $\theta = 0^o$, by πR. These can be checked with the critical buckling moment expression used by Ref. 35,

$$M_{cr} = EI \left\{ \frac{0.6\ t/R \ - \ 10^{-7} R/t}{1 \ + \ 0.004\ E/f_y} \right\} \qquad (10.1)$$

where

E = Young's modulus,

I = section modulus,

t = cylinder thickness,

R = cylinder radius,

and

f_y = structural yield stress.

The check indicated significant conservatism in the structure for the present level of seismic resistance sought.

Table 10.3 Comparison of Frequencies (Hz) of the Water Tower

Case \ Mode	1	2	3	4	5	6	7	8
I	0.503	2.99	14.05	20.97	26.30	27.34	30.91	31.88
II	0.440	2.99	14.03	19.82	22.83	27.24	28.93	30.93
III	0.372	2.92	14.03	18.61	22.15	26.04	27.30	30.93
IV	0.301	2.04	13.44	15.83	18.45	19.61	21.50	25.25

Table 10.4 Foundation Reactions, and Radial Displacements at Nodes 15 and 17 for $\theta = 0^{\circ}$, at $t = 3.4$ s.

Case	Axial Force kN/m	Tang. Force kN/m	Rad. Force kN/m	Axial Moment kNm/m	Node	w mm
I	89.1	6.4	20.8	-9.7	15 17	-7.44 -7.24
II	84.9	6.2	19.8	-9.2	15 17	-7.05 -6.88
III	80.7	5.9	18.9	-8.8	15 17	-6.68 -6.53
IV	76.6	5.8	17.8	-8.3	15 17	-6.33 -6.20

Table 10.5 Tank Stresses at Midpoints of Elements 15 and 17 for $\theta = 0^{\circ}$, at $t = 12.1$ s

Case	Element	N_s kN/m	N_θ kN/m	M_s kNm/m	M_θ kNm/m
I	15	5.7	-2.3	0.26	0.08
	17	12.6	-40.3	-1.05	-0.35
II	15	5.7	2.7	0.34	0.10
	17	12.7	-37.6	-0.97	-0.33
III	15	5.5	2.6	0.32	0.10
	17	12.1	-36.0	-0.93	-0.33

CHAPTER 11

CONCLUSION AND DISCUSSION

11.1 Conclusions

The following conclusions are drawn from this study :

i) Free vibration frequencies of the elevated water tank decrease as the water depth is increased.

ii) Elevated water tank frequencies are higher when sloshing is permitted.

iii) The liquid sloshing effect tends to cause relatively larger stresses at the tank wall and smaller values at the supporting structure.

iv) When partially filled with water, the first mode damping ratio of the elevated tank system may be dominated by the damping ratio of the liquid motion. This causes a considerable reduction in the system damping ratio, consequently amplifying the response of the structure to ground excitation.

11.2 Discussion

Although the theory used in this method is rigorous, the procedure is straightforward for seismic response analysis of axisymmetric liquid storage structures. However, the discretisation of the structure into elements requires judgment, particularly where there are high gradients in the profile. For partially filled elevated tanks, it may be desirable to use a larger number of mode shapes. The operating conditions of the tank (e.g. constant head supply or partially full conditions), and the level of seismic resistance sought are necessary pre-analysis specifications.

The effect of the tilting action of the tank base has to be considered for thin-walled tanks (e.g. steel tanks) for high seismicity. This can partly be done by generalising the formulation to include higher circumferential harmonics in the simulation of load excitation. The work can be extended to include the conical shape of the tank bottom. Nonlinear effects of liquid sloshing can also be considered.

BIBLIOGRAPHY

1. DuVall, W., 'Approximate Models for Offshore Concrete Gravity Structures', M.S. Thesis, Massachusetts Institute of Technology, 1976

2. Glacel, R. A., 'Reduction of Offshore Platform Dynamic Response by Tuned Mass Damper', M.S. Thesis, Massachusetts Institute of Technology, 1977

3. Housner, G. W., 'Dynamic Pressure on Accelerated Fluid Containers', Bull. Seism. Soceity of America, Vol. 47, No 1, 15-36 (1957)

4. Stephens, D. G., Leonard, H. W., and Silveira, M. A., ' An Experimental Investigation of the Damping of Liquid Oscillations in an Oblate Spheroidal Tank With and Without Baffles', NASA TN D-808, 1961

5. Skjelbreia, L. and Hendrickson, J. A., 'Fifth Order Gravity Wave Theory', Proceedings of 7th Conference on Coastal Engineering, Tokyo, 1960. Council on Wave Research, Richmond, California, 184-196 (1961)

6. Myers, J. J., Holm, C. H., McAllister, R. F., Handbook of Ocean and Underwater Engineering, McGraw-Hill, New York, 1969

7. Evans, D. J., 'Analysis of Wave Force Data', Proc. Offshore Technology Conference, Houston, Texas, Paper 1005, 51-70 (1969)

8. Hudspeth, R. T., Dalrymple, R. A., and Dean, R. G., 'Comparison of Wave Forces Computed by Linear and Stream Function Methods', Proc. Offshore Technology Conference, Houston, Texas, Paper 2037, 17-32 (1974)

9. Kinsman, B., Windwaves, Prentice-Hall, New York, 1965.

10. Pierson, W. and Moskowitz, L., 'A Proposed Spectral Form for Fully Developed Wind Seas Based on the Similarity Theory of S. A. Kitaigorodskii', Journal of Geophysical Research, Vol. 69, 5181-5190 (1964)

11. Korzhavin, K. N., 'Action of Ice on Engineering Structures', Novosibirsk, USSR, 1962. English Translation, Cold Regions Research in Engineering Laboratory, 319 pp. (1971)

12. Zubov, N. N., 'Artic Ice', Izdatel 'Stvo Glavsevmoi eti, Moscow (1945). Translation by the U.S. Navy Oceanographic Office and the American Metorological Soceity, 489 pp. (1963)

13. Blenkarn, K. A. and Knapp, A. E., 'Ice Conditions on the Grand Banks', Ice Seminar Sponsored by Petroleum Soceity of Canadian Institute of Mining and Metallurgy, and the American Petroleum Institute, Calgary, Alberta, 61-72 (1969)

14. Kopaigorodski, E. M., Vershinin, S. A., and Nifontov, S. A., 'Model Investigations of the Effect of an Ice Field Pushed Against the Piles of Offshore Oil Platforms, IAHR/AIRH Symp. on Ice and Its Action on Hydraulic Structures, Leningrad, U.S.S.R., 100-102 (1972)

15. Blumberg, R. and Strader, N. R. II, 'Dynamic Analysis of Offshore Structures', Proc. Offshore Technology Conference, Houston, Texas, Paper 1009, 107-126 (1969)

16. Reddy, D. V., Cheema, P. S., and Swamidas, A. S. J., Ice Force Response Spectrum Modal Analysis of Offshore Towers', Proc. Third POAC Conference, University of Alaska, Alaska, 304-314 (1975)

17. Swamidas, A. S. J. and Reddy, D. V., 'Dynamic Ice Structure Interaction of Offshore Monopod Towers by Hybridisation of the Computer Programs EATSW and SAP-IV', Proc. First SAP-IV User's Conference, Los Angeles, California, 33 pp. (1976)

18. Den Hartog, J. P., Mechanical Vibrations, McGraw-Hill, New York, 1956.

19. Morrow, C. T., Troesch, B. A., and Spence, H. R., 'Random Response of Two Coupled Resonators Without Loading', J. Acoust. Soc. Am., Vol. 33, 46-55 (1961)

20. Gupta, Y. P. and Chandrasekaran, A. R., 'Absorber System for Earthquake Excitations', Proc. 4th World Conf. Earthquake Engineering, Santiago, Chile, 1969.

21. Wirsching, W. T. and Yao, J. T. P., 'Modal Response of Structures', J. Struct. Div., ASCE, Vol. 96, 879-883 (1970)

22. Crandall, S. H. and Mark, W. D., Random Vibration in Mechanical Systems, Academic Press, New York, 1963

23. Wirsching, W. T. and Campbell, G. W., 'Minimal Structural Response Under Random Excitation Using the Vibration Absorber', Earthquake Engineering and Structural Dynamics, Vol. 2, 303-312 (1974)

24. McNamara, R. J., 'Tuned Mass Dampers for Buildings', J. Struct. Div., ASCE, Vol. 103, 1785-1798 (1977)

25. Brock, J. E., 'A Note on Damped Vibration Absorber', Trans. ASME, A284 (1946)

26 Miles, J. W., 'Ring Damping of Free Surface Oscillations in a Circular Tank', J. Appl. Mech., Vol. 25, 274-276 (1958)

27. Siekmann, J. and Chang, S. C., 'On the Change of Natural Frequencies of a Sloshing Liquid by Movable Devices', Acta Mech., Vol. 11, 73-86 (1971)

28. Miner, M. A., 'Cumulative Damage in Fatigue', J. Appl. Mech., Vol. 12, 159-164 (1945)

29. Masubuchi, K., Materials fo Ocean Engineering, MIT Press, Cambridge, 1970

30. Hill, R. K. and Biggs, K. L., 'Water Storage Tanks in Seismic Areas of Papua New Guinea', Report 31, Div. Bldg. Research, Commonwealth Scientific and Industrial Organisation, Australia, 1974

31. Veletsos, A. S. and Yang, J. Y., 'Earthquake Response of Liquid-Storage Tanks', Advances in Civil Engineering Through Engineering Mechanics, Proc. Annual EMD Spec. Conf., Raleigh, ASCE, 1-24, (1977)

32. Balendra, T. and Nash, W. A., 'Earthquake Analysis of a Cylindrical Liquid Storage Tank With a Dome by Finite Element Method', University of Massachusetts Report to the National Science Foundation, ENV-76-14833-1, May 1978

33. Jacobsen, L. S., 'Impulsive Hydrodynamics of Fluid Inside a Cylindrical Tank and of a Fluid Surrounding a Cylindrical Pier', Bull. Seism. Soc. America, Vol. 39, 189-204 (1949)

34. Jacobsen, L. S. and Ayre, R. S., 'Hydrodynamic Experiments with Rigid Cylindrical Tanks Subjected to Transient Motions', Bull. Seism. America, Vol. 41, 313-347 (1951)

35. Shepherd, R., 'Earthquake Resistant Design of Petroleum Storage Tanks', Proc. 2nd Australasian Conf. on the Mechanics of Structures and Materials, University of Adelaide, 8.1-8.16 (1969)

36. Lindholm, J. S., Kana, D. D., and Abramson, H. N., 'Breathing Vibrations of a Circular Cylindrical Shell with an Internal Liquid', J. Aerospace Science, Vol. 29, 1052-1059 (1962)

37. Chu, W. H., 'Breathing Vibrations of a Partially Cylindrical Tank - Linear Theory', J. Appl. Mech., Vol 30, 532-536 (1963)

38. Kana, D. D. and Chu, W. H., 'Influence of Rigid top Mass on Response of Pressurised Cylinder Containing Liquid', J. Spacecraft and Rockets, Vol. 6, 103-110 (1969)

39. DiMaggio, F. L. and Bleich, H. H., 'Dynamic Response of a Containment Vessel to Fluid Pressure Pulses', Computers and Structures, Vol. 8, 31-39 (1978)

40. Fung, Y. C., Sechler, E. E., and Kaplan, A., 'On Vibrations of Thin Shells Under Internal Pressures', J. Aeron. Sc., Vol.27, 650-61(1957)

41. Luk, C. H., 'Finite Element Analysis for Liquid Sloshing Problems', Report ASRL-TR-144-3, Aeroelastic and Structures Laboratory, Massachusetts Institute of Technology, Cambridge, 1969

42. Edwards, N. W., 'A Procedure for the Dynamic Analysis of Thin Walled Cylindrical Liquid Storage Tanks Subjected to Lateral Ground Motions', Phd. Dissertation, University of Michigan, Ann Arbor, 1969

43. Bauer, H. F. and Siekmann, J., 'Dynamic Interaction of a Liquid with the Elastic Structure of a Circular Cylindrical Container', Ing-Arch, Vol. 40, 266-280 (1971)

44. Wu, C. I., Mouzakis, T., Nash, W. A., and Colonell, J. M., 'Natural Frequencies of Cylindrical Liquid Storage Containers', University of Massachusetts Report to the National Science Foundation, GI 39644-1, 1975

45. Shaaban, S. H. and Nash, W. A., 'Finite Element Analysis of a Seimically Excited Cylindrical Storage Tank, Ground Supported, and Partially Filled with Liquid', University of Massachusetts Report to the National Science Foundation, 1976

46. Clough, D. P. and Clough, R. W., 'Earthquake Simulation Studies of Liquid-Filled Cylindrical Tanks', Nuclear Engineering and Design, 446, 367-380 (1978)

47. Carder, D. S., 'Observed Vibration of Steel Water Towers', Bull. Seism. Soc. America, Vol. 26(1), 69-88 (1936)

48. Ruge, A. C., 'Earthquake Resistance of Elevated Water Tanks', Trans. ASCE, 889-949 (1938)

49. Cloud, W. K., 'Period Measurements of Structures in Chile', Bull. Seism. Soc. America, Vol. 53, 381-387 (1963)

50. Blume, J. A., 'A Structural-Dynamic Analysis of Steel Plant Structures Subjected to the May 1960 Chilean Earthquake', Bull. Seism. Soc. America, Vol. 53, 439-480 (1963)

51. Chandrasekaran, A. R. and Krishna, J., 'Water Tanks in Seismic Zones', Proc. 3WCEE, New Zealand, Vol. IV,161-171 (1954)

52. Sonobe, Y. and Nishikawa, T., 'Study on the Earthquake Proof Design of Elevated Water Tanks, Proc. 4WCCE, Santiago, B4, 11-24 (1969)

53. Ifrim, M. and Bratu, C., 'The Effect of Seismic Action on the Dynamic Behaviour of Elevated Water Tanks', Proc. 4WCEE, Santiago, B4, 127-142 (1969)

54. Garcia, S. M., 'Earthquake Response Analysis and Seismic Design of Cylindrical Tanks, Proc. 4WCEE, Santiago, B4, 169-182 (1969)

55. Shepherd, R., 'Two Mass Representation of a Water Tower Structure', J. Sound and Vibration, Vol. 23(3), 391-396 (1972)

56. Tillerson, J. R. and Haisler, W. E., 'SAMMSOR-II, A Finite Element Program to Determine Stiffness and Mass Matrices of Shells of Revolution', Texas A & M University, College Station, Oct. 1970

57. Stricklin, J. A., Navaratna, D. R., and Pian, T. H. H., 'Improvement on the Analysis of Shells of Revolution by Matrix Displacement Method', AIAA Journal, Vol. 4(11), 2069-2072 (1966)

58. Hsiung, H. C. H. and Weingarten, V. I., 'Dynamic Analysis of Hydroelastic Systems Using the Finite Element Method', Department of Civil Engineering, University of Southern California, Report USCCE 013, Nov. 1973

59. Zienkiewicz, O. C., The Finite Element Method, McGraw-Hill, New York, 542-543, 1977

60. Clough, R. W. and Penzien, J., Dynamics of Structures, McGraw-Hill, New York, 576-577, 1975

COMPUTER DOCUMENTATION

```
*************************************************************************************
   This computer program is a modified version of the program originally developed by
   DuVall, and later extended by Glacel.  The program consists of the dynamic analysis
   of an axisymmetric offshore tower carrying a deck mass, subjected to digitised
   wave spectral input.  The available options are:
        1)   Dynamic analysis without vibration absorber
        2)   Dynamic analysis with a tuned mass damper
        3)   Dynamic analysis with a liquid vibration absorber
*************************************************************************************
      IMPLICIT REAL*8(A-H,O-Z)
      DOUBLE PRECISION MASS,LENGHT
      COMPLEX A,B
      DIMENSION TOWER (20), FREQ (100), MASS(200), STIFF(200),A(200),
     *B(50),DIS(50),VEL(50),ACC(50),R(50),S(50),H(50),PHASE(50),Q(500),
     *P(50)
      DIMENSION EL(2)
      DATA IR,IW/5,6/
      CALL INPUT (IR,IW,TOWER,NELEM,NFREQ,
     *HEIGHT,ZO,REB,RET,RIB,RIT,DEPTH,E,RO,DMASS,DINER,FREQ,
     *H,PHASE,DT,TIME,NRIGD ,KQ,KD,KM,ALPHA,BETAV,BETAH,DK,DM,BETAD,KNW,
     *TM,TMO,EL,ET,THICK,RAD)
      CALL ASMBL (NELEM,NEQ,MBW,
     *HEIGHT,REB,RET,RIB,RIT,E,RO,DMASS,DINER,STIFF,MASS,KQ,
     *NRIGD,IR,IW,DEPTH,KD,DM,DK,KM,LENGHT,DA,DB,TM,TMO,EL,ET,THICK,RAD)
      NFREQ=-NFREQ
      CALL TF(IW,TOWER,NELEM,HEIGHT,ZO,RET,REB,DEPTH,
     *NEQ,MBW,STIFF,MASS,A,B,FREQ,KQ,NRIGD ,H,BETAV,BETAH,ALPHA,
     *KD,LENGHT,DA,DB,RIT,S,BETAD,DK,DM,NFREQ,KNW)
      STOP
      END
      SUBROUTINE INPUT(IR,IW,TOWER,NELEM,NFREQ,
     *HEIGHT,ZO,REB,RET,RIB,RIT,DEPTH,E,RO,DMASS,DINER,FREQ,
     *H,PHASE,DT,TIME,NRIGD,KQ,KD,KM,ALPHA,BETAV,BETAH,DK,DM,BETAD,KNW,
     *TM,TMO,EL,ET,THICK,R)
      IMPLICIT REAL*8(A-H,O-Z)
      COMMON/HT/HOL,H1L
      DIMENSION EL(2)
      DIMENSION TOWER(20),FREQ(1),H(1),PHASE(1)
C
      READ(IR,1) TOWER,NELEM,NFREQ,NRIGD,KQ,KD,KM,KNW
      WRITE(IW,2)TOWER,NELEM,NFREQ
      IF(KQ.NE.0)WRITE(IW,50)
 50   FORMAT(///5X, 'EARTHQUAKE OPTION IN EFFECT')
      IF(KD.GT.0)WRITE(IW,51)
      IF(KD.LT.0)WRITE(IW,52)
 51   FORMAT(//5X, 'DAMPER OPTION IN EFFECT')
 52   FORMAT(//5X, ' LIQUID SLOSHING DAMPER IN EFFECT ')
C
C ##  READ OVERALL DIMENSIONS
      READ(IR,3) HEIGHT,ZO,REB,RET,RIB,RIT,DEPTH
      WRITE(IW,4)HEIGHT,ZO,REB,RET,RIB,RIT,DEPTH
C ##  READ MATERIAL PROPERTIES
      READ(IR,3) E,RO
```

```
      WRITE(IW,5)E,RO

 ##   READ ALPHA,BETAV,BETAH FOR DAMPING. IF NO DAMPING READ IN ZERO VAL
      READ (IR,3) ALPHA,BETAV,BETAH
      WRITE(IW,21)ALPHA,BETAV,BETAH

 ##   READ DECK LOAD
      READ (IR,3) DMASS ,DINER
      WRITE(IW,6) DMASS ,DINER
      IF(KD.EQ.0)GO TO 22
      IF(KD.LT.0)GO TO 23
      READ(IR,41)DM,OMEGA,BETAD
      DK=OMEGA **2 * DM
      WRITE(IW,42) DK,DM,OMEGA,BETAD
41    FORMAT(3F8.4)
42    FORMAT(4X, 'DAMPING PARAMETERS'/2X, 'SPRING CONSTANT=',F10.4/2X,
     * 'DAMPER MASS =',F8.4 /2X, 'DAMPER FREQUENCY(RAD/SEC) =',F8.4/
     *2X, 'PERCENT CRITICAL DAMPING =',F8.4)
      GO TO 22
23    CONTINUE
      READ(IR,3)R,HL,ROL,ET,BETAD,THICK
      WRITE(IW,1000)R,HL,ROL,ET,THICK
1000  FORMAT(2X,5E20.8)
      CALL SLOSH(R,HL,ROL,9.81D0,TM,TMO,DM    ,EL,OMEGA )
      DK=OMEGA**2*DM
      WRITE(IW,30)TMO,DM,DK,HOL   ,H1L   ,OMEGA,BETAD
30    FORMAT(4X, 'DAMPING PARAMETERS'/2X,' IMPULSIVE MASS = ',F10.4/2X,
     *' CONVECTIVE MASS = ',F8.4/2X,' EQUIVALENT SPRING CONSTANT = ',
     *F10.4/2X,' HO = ',F10.4/2X,' H1 =',F10.4/2X,' DAMPER FREQUENCY(RAD
     */SEC) = ',F10.4/2X,'PERCENT CRITICAL DAMPING = ',F10.4)
22    CONTINUE
 ##   READ FREQUENCIES
      IF (NFREQ.GE.0) GO TO 10
 ##   READ FREQUENCIES FOR STATIC RESPONSE IN FREQUENCY DOMAIN
      N = -NFREQ
      READ (IR,3)(FREQ(I),H(I),I=1,N)
      WRITE(IW,7)(FREQ(I),H(I),I=1,N)
      RETURN
 ##   READ TIME AND TIME INTERVAL PLUS CONDENSED SPECTRUM PARAMETERS
 ##   FOR DYNAMIC ANALYSIS
10    IF(NFREQ.LE.0)GO TO 12
      READ(IR,3)DT,TIME
      WRITE(IW,8)DT,TIME
      DO 11 I=1,NFREQ
11    READ (IR,3)FREQ(I),H(I),PHASE(I)
      WRITE(IW,9)(FREQ(I),H(I),PHASE(I) ,I=1,NFREQ)
12    RETURN

1     FORMAT(20A4,/,7I4)
2     FORMAT('1',/,5X,20A4,//,
     * 5X,I5, 'ELEMENTS',/,5X,I5,'FREQUENCIES',/)
3     FORMAT(8F10.2)
4     FORMAT(///5X, '*OVERALL DIMENSIONS*'//
     *5X, 'TOWER HEIGHT     ',F8.2, 'M.' /
     *5X, 'CAISSON HEIGHT  ', F8.2,'M.' / /
     *5X, 'EXTERNAL RADIUS AT THE BOTTOM  ',F7.2,  'M.'/
```

```
*5X, 'EXTERNAL RADIUS AT THE TOP      ',F7.2,  'M.'/
*5X, 'INTERNAL RADIUS AT THE BOTTOM   ',F7.2,  'M.'/
*5X, 'INTERNAL RADIUS AT THE TOP      ',F7.2,  'M.'/
*5X, 'DEPTH OF WATER  ',F8.2, 'M.' / )
 FORMAT(///5X, '*MATERIAL PROPERTIES*'//
*5X, 'E =', E10.3/5X,'RO =', E10.3 /)
 FORMAT (///5X, 'DECK MASS    ', E12.4 /
*          5X, 'DECK INERTIA', E12.4 /)
 FORMAT(///5X,'CONDENSED SPECTRUM PARAMETERS *' ///3X,' FREQ',8X,
*'WAVE HEIGHT'//(3X,2F15.4))
 FORMAT(///5X, '* TIME INTERVAL AND TOTAL TIME * '//5X,
*'DELTA T =  ',F7.3/5X, 'TIME  = ' , F7.3/ )
 FORMAT ( ///5X, '* CONDENSED SPECTRUM PARAMETERS  *'//13X,
*'FREQ' , 8X , 'WAVE HEIGHT' , 3X , 'PHASE ANGLE' //(3X, 3F15.4))
 FORMAT(///5X, ' * DAMPING COEFFICIENTS *'//5X, 'ALPHA= ',E10.3/5X,
*'BETAV = ',E10.3 /5X,'BETAH= ', E10.3/)
 END
 SUBROUTINE SLOSH(R,HL,ROL,G,TM,TMO,TM1,     EL,OMEGA)
 IMPLICIT REAL*8(A-H,O-Z)
 COMMON/HT/HOL,H1L
 DIMENSION EL(2)
 TM=3.14159*R*R*HL*ROL
 A=R/HL
 B=HL/R
 F1=DCOSH(1.732*A)
 F2=DSINH(1.732*A)
 F3=DCOSH(1.837*B)
 F4=DSINH(1.837*B)
 TMO=TM/(1.732*A)*DSINH(1.732*A)/DCOSH(1.732*A)
 TM1=0.21*TM*1.837*A*F4/F3
 HOL=0.375*HL*(1.0+1.33*(1.732*A*F1/F2-1.0))
 H1L=HL*(1.0-(F3-1.534)/(1.837*B*F4))
 OMEGA=(G/R)*1.837*F4/F3
 OMEGA=DSQRT(OMEGA)
 IF(H1L.LE.HOL)GO TO 1
 EL(1)=HOL
 EL(2)=H1L-HOL
 GO TO 3
 IF(H1L.EQ.HOL)GO TO 2
 EL(1)=H1L
 EL(2)=HOL-H1L
 GO TO 3
 EL(1)=HOL
 EL(2)=0.1
 CONTINUE
 RETURN
 END
 SUBROUTINE ASMBL (NELEM, NEQ, MBW,
*HEIGHT, REB, RET, RIB, RIT, E, RO, DMASS, DINER, STIFF, MASS, KQ,
*NRIGD,IR,IW,DEPTH,KD,DM,DK,KM,LENGHT,DA,DB,TM,TMO,EL,ET,THICK,R)
 IMPLICIT REAL*8(A-H,O-Z)
 DOUBLE PRECISION MASS,LENGHT,MG
 COMMON/HT/HOL,H1L
 DIMENSION STIFF(200),MASS(200),A(15),AMAS(19,19),STIF(19,19)
 DIMENSION EL(2)
```

```
#    INITALIZE
     NEQ= 2*(NELEM + 1)
     IF(KQ.NE.0) NEQ=NEQ+2
     IF(KD.NE.0) NEQ=NEQ+1
     IF(KD.LT.0)NEQ=NEQ+4
     MBW=5
     LIM=NEQ*MBW
     DO 10 I=1,LIM
     STIFF(I)=0.0
  10 MASS(I) =0.0

##   COMPUTE ELEMENT MATRICES AND ASSEMBLE
     DN=NELEM
     LENGHT = HEIGHT/DN
     DA=(RET-REB)/DN
     DB=(RIT-RIB)/DN
     A1 = REB
     B1=RIB
     EMASS=DMASS
     IF(KD.GT.0) EMASS=EMASS + DM
     IF(KD.LT.0)EMASS=EMASS+TM

     DO 12 N=1,NELEM
     A2 = A1 + DA
     B2 = B1 + DB
     CALL SUBK (E,A1,B1,A2,B2,LENGHT,A)
     CALL ADD (NEQ,STIFF,N,A)
     CALL SUBM (RO,A1,B1,A2,B2,LENGHT,EMASS,A )
     CALL ADD (NEQ,MASS,N,A)
     A1 = A2
2    B1 = B2
     A11=R+THICK
     B11=R
     K=0
     N1=NELEM+1
     N2=NELEM+2
     DO 201 N=N1,N2
     K=K+1
     DIS   =EL(K)
     CALL SUBK(ET,A11,B11,A11,B11,DIS,A)
01   CALL ADD(NEQ,STIFF,N,A)

##   ADD DECK MASS
     I=2 * NELEM
     MASS(I+1) = MASS(I+1) + DMASS
     MASS(I+2) = MASS(I+2) + DINER
     IF(KD.GE.0)GO TO 1
     IF(H1L.GE.HOL)MASS(I+3)=TMO
     IF(H1L.LT.HOL)MASS(I+5)=TMO
     CONTINUE

     A1 = REB
     B1 = RIB
     DO 14 M=1,NELEM
     A2 = A1 + DA
     B2 = B1 + DB
```

```
      CALL SUBKG(RO,REB,RIB,A1,B1,A2,B2,LENGHT,EMASS,M,A)
      CALL ADD(NEQ,STIFF,M,A)
      A1 = A2
14    B1 = B2
      IF (KD.EQ.0) GO TO 40
      IF(KD.GT.0)GO TO 38
##    MODIFY MATRICES FOR MASS DAMPER
      IF(H1L.LT.HOL)GO TO 39
      GO TO 38
9     CONTINUE
      I=NEQ-4
      J=NEQ
      K=5*NEQ-4
      GO TO 41
8     CONTINUE
      I=NEQ-2
      J=NEQ
      K=3 * NEQ - 2
1     CONTINUE
      STIFF(I) = STIFF(I) + DK
      STIFF(J)=DK
      STIFF(K)=-DK
      MASS(J)=DM
0     CONTINUE
      IF(KM.EQ.0)GO TO 43
##    PRINT OUT MASS AND STIFFNESS MATRICES
      WRITE(IW,29)
29    FORMAT(//10X, ' MASS MATRICES'//)
      DO 100 I=1,NEQ
      DO 75  J=1,NEQ
75    AMAS(I,J)=0.0
100   CONTINUE
      DO 101 I =1,NEQ
      K=I+4
      DO 76 J=I,K
      IJ=(J-I) * NEQ + I
76    AMAS(I,J)=MASS(IJ)
101   CONTINUE
      DO 102 I=1,NEQ
      K=I+1
      L=I+4
      DO 77 J=K,L
77    AMAS(J,I)=AMAS(I,J)
102   CONTINUE
      DO 30 I=1,NEQ
      WRITE(IW,27)(AMAS(I,J),J=1,NEQ)
31    FORMAT(/1X,15E8.1)
30     CONTINUE
      WRITE(IW,32)
32    FORMAT(//10X, 'STIFFNESS MATRIX'//)
      DO 103 I=1,NEQ
      DO 78 J=1,NEQ
78    STIF(I,J)=0.0
03    CONTINUE
      DO 104 I=1,NEQ
      K=I+4
```

```
   DO 79 J=I,K
   IJ=(J-I)*NEQ+I
   STIF(I,J)=STIFF(IJ)
   CONTINUE
   DO 105 I=1,NEQ
   K=I+1
   L=I+4
   DO 80 J=K,L
   STIF(J,I)=STIF(I,J)
 5 CONTINUE
   DO 28 I=1,NEQ
   WRITE(IW,27)(STIF(I,J),J=1,NEQ)
   FORMAT(/11E10.3)
   CONTINUE
 3 RETURN
   END
   SUBROUTINE SUBK (E,A1,B1,A2,B2,LENGHT,STIFF)
   IMPLICIT REAL*8(A-H,O-Z)
   DOUBLE PRECISION MASS,LENGHT
   DIMENSION A(5),W(5),F(4),STIFF(15)
   DATA A,W/0.0D0,-0.538469D0,0.538469D0,-0.906180D0,0.906180D0 ,
  *0.568889D0,2*0.478629D0,2*0.236927D0/
   DO 1 I=1,15
   STIFF(I)=0.
   DO 2 N=1,5
   X=A(N)
   X=0.5 * (X+1.0)
   F(1)=12.0*X-6.0
   F(3)=-F(1)
   F(2)= (-4.0 + 6.0*X) * LENGHT
   F(4)= (-2.0 + 6.0*X) * LENGHT
   AA = A1*(1.0 - X) + A2*X
   B  = B1*(1.0 - X) + B2*X
   C = 0.7853981*(AA**4 - B**4)/LENGHT**3/2.0*W(N)*E
   IJ=0
   DO 2 J=1,4
   DO 2 I=1,J
   IJ=IJ+1
   STIFF(IJ)=STIFF(IJ) + C*F(I)*F(J)
   RETURN
   END
   SUBROUTINE ADD (NEQ,A,N,B)
   IMPLICIT REAL*8(A-H,O-Z)
   DIMENSION A(1),B(1)
   NN=2*(N-1)
   KL=0
   DO 10 J=1,5
   DO 10 I=1 ,J
   II=J-I
   IJ=NEQ*II + NN + I
   KL=KL+1
   A(IJ)=A(IJ) + B(KL)
   RETURN
   END
   SUBROUTINE SUBM  (RO,A1,B1,A2,B2,LENGHT,EMASS,MASS)
   IMPLICIT REAL*8(A-H,O-Z)
```

```
      DOUBLE PRECISION MASS,LENGHT
      DIMENSION A(5),W(5),F(4),MASS(15)
      DATA A,W/0.0D0,-0.538469D0,0.538469D0,-0.906180D0,0.906180D0 ,
     *0.568889D0,2*0.478629D0,2*0.236927D0/
      DO 1 I=1,15
      MASS(I)=0.0
      DO 2 N=1,5
      X=A(N)
      X=0.5*(X+1.0)
      F(3)= X*X*(3.0 - 2.0*X)
      F(1)= 1.0 - F(3)
      F(4)= X * X * LENGHT * (X-1.0)
      F(2)= X * LENGHT * (1.0 - 2.0*X + X*X)
      AA = A1 * (1.0 - X) + A2 * X
      B = B1 * (1.0 - X) + B2 * X
      C=3.14159265 * (AA * AA - B*B) * RO * LENGHT /2.0 * W(N)
      EMASS = EMASS + C
      IJ=0
      DO 2 J=1,4
      DO 2 I=1,J
      IJ=IJ+1
      MASS(IJ)=MASS(IJ) + C * F(I) * F(J)
      RETURN
      END
      SUBROUTINE SUBKG(RO,REB,RIB,A1,B1,A2,B2,LENGHT,EMASS,M,STIFG)
      IMPLICIT REAL*8(A-H,O-Z)
      DOUBLE PRECISION MASS,LENGHT
      DIMENSION A(5),W(5),F(4),STIFG(15)
      DATA A,W/0.0D0,-0.538469D0,0.538469D0,-0.906180D0,0.906180D0 ,
     *0.568889D0,2*0.478629D0,2*0.236927D0/
      DM=M-1
      DO 1 I=1,15
      STIFG(I)=0.
      DO 2 N =1,5
      X=A(N)
      X=0.5 * (X+1.0)
      F(1)=X*6.0*(X-1.0)
      F(2)=(1.0-4.0*X + 3.0*X*X) * LENGHT
      F(3)=-F(1)
      F(4)=(3.0*X - 2.0) * LENGHT*X
      A3 = (A2-A1) * X + A1
      B3 = (B2-B1) * X + B1
      QMASS=RO * 3.14159265 * (DM + X) * LENGHT/3.0 * ((REB*REB
     *+ A3 * REB + A3 * A3) - (RIB*RIB + B3*RIB + B3*B3))
      P=9.81*(EMASS - QMASS) / LENGHT*W(N) / 2.0
      IJ=0
      DO 2 J=1,4
      DO 2 I=1,J
      IJ = IJ+1
      STIFG(IJ)=STIFG(IJ) + P*F(I)*F(J)
      RETURN
      END
      SUBROUTINE TF(IW,TOWER,NELEM,HEIGHT,ZO,RET,REB,DEPTH,
     *NEQ,MBW,STIFF,MASS,A,B,FREQ,KQ,NRIGD,H,BETAV,BETAH,ALPHA,
     *KD,LENGHT,DA,DB,RIT,S,BETAD,DK,DM,NFREQ,KNW )
      IMPLICIT REAL*8(A-H,O-Z)
```

```
      DOUBLE PRECISION MASS,LENGHT
      COMPLEX*16 A,B,C,G,F,T,R,Q
      DIMENSION TOWER(20),STIFF(1),MASS(1),A(1),B(15),P(4),S(1),US(15),
     *VS(15),HS(15),SS(5),FREQ(1),H(1)
      J=NELEM+1
      DO 100 I=1,J
      US(I)=0.
      VS(I)=0.
      HS(I)=0.
00    SS(I)=0.
      USD=0.
      HSD=0.
      DO 99 L=1,NFREQ
      W=6.28318531 * FREQ(L)
      W2=W*W

##    FORM COEFFICIENT MATRIX
      LIM=NEQ*MBW
      D=W*BETAV + 2.0*BETAH
      G=DCMPLX(1.0D0,D)
      F=DCMPLX(-W2,W*ALPHA)
      DO 1 I=1,LIM
      A(I)=G*STIFF(I) + F*MASS(I)

      IF(KD.EQ.0)GO TO 15
      CD=W*2.0*BETAD*DSQRT(DK)*DSQRT(DM)
      T=DCMPLX(0.0D0,CD-D*DK)
      R=DCMPLX(0.0D0,-CD+D*DK)
      X=D*DK+W*ALPHA*DM
      Q=DCMPLX(0.0D0,CD-X)
      A(NEQ-2)=A(NEQ-2)+T
      A(NEQ)=A(NEQ)+Q
      A(3*NEQ-2)=A(3*NEQ-2)+R
15    CONTINUE

##    FORM LOAD VECTOR
      DO 2 I=1,NEQ
      B(I)=0.
      DN=NELEM
      LENGHT=HEIGHT/DN
      DA=(RET-REB)/DN
      A1=REB
      DO 4 N=1,NELEM
      A2=A1+DA
      CALL SUBP(N,A1,A2,LENGHT,ZG,DEPTH,W2,P)
      J=2*(N-1)
      DO 3 I=1,4
      J=J+1
       C=P(I)*H(L)
      B(J)=B(J)+C
      A1=A2

##    IMPOSE DISPLACEMENT BOUNDARY CONDITIONS
      IF(NRIGD.EQ.0)GO TO 9
      DO 5 I=1,LIM,NEQ
      A(I)=0.0
```

```
   A(I+1)=0.
   B(1)=0.0
    B(2)=0.0

   SOLVE SYSTEM OF EQUATIONS
   CALL SOLVE(0,IW,NEQ,MBW,1,A,B,LIM,NELEM,RET,RIT,LENGHT,DA,DB,S)

   PRINT OUT STEADY-STATE RESPONSE
   GO TO 103
   IF(KNW.NE.0)GO TO 103
   REQ=FREQ(L)
   WRITE(IW,6)TOWER,REQ
3  CONTINUE
   I2=NEQ
   IF(KD.EQ.0)GO TO 10
   HACC=-(CDABS(B(I2))*W2)
   Y=CDABS( B(I2) - B(I2-2) )
   USD=USD + Y**2
   HSD = HSD + HACC**2
   GO TO 101
   IF(KNW.NE.0)GO TO 101
   WRITE(IW,11)Y,HACC
1  FORMAT(13X, E15.5, 21X, E15.5)
1  CONTINUE
   I2=I2-1
   IF(KD.LT.0)I2=I2-4
   CONTINUE
   NNODE=NELEM+1
   DO 7 I=1,NNODE
   J=NNODE-I+1
   HACC=-(CDABS ( B(I2-1)) * W2)
   U=CDABS(B(I2-1) )
   V=CDABS(B(I2) )
   US(J)=US(J) + U**2
   VS(J)=VS(J) + V**2
   HS(J)=HS(J) + HACC**2
   U=U/6.6402
   IF(KNW.NE.0)GO TO 102
   IF(I.EQ.1)WRITE(IW,8)J,U,V,HACC
2  CONTINUE
   I2=I2-2
   FORMAT('1' /5X,20A4//5X,'*STEADY-STSTE RESPONSE AT ',F8.3, ' CPS*'
  *//5X,'NODE',6X, 'DISPLACEMENT',10X, 'ROTATION',10X, 'ACCELERATION'
  */ )
   FORMAT(5X,I4, 3(3X,E15.5) )
   IF (KNW.NE.0 )GO TO 104
   WRITE (IW,12)REQ
4  CONTINUE
   FORMAT(/////5X,'*ELEMENT STRAINS AT ',F8.3, ' CPS*'//5X,'ELEMENT',
  *6X, 'STRAIN' / )
   DO 13 I=1,NELEM
   SS(I)=SS(I) + S(I)**2
   IF(KNW.NE.0)GO TO 105
   WRITE(IW,14)I,S(I)
   FORMAT(5X,I4,3X,E15.5)
5  CONTINUE
```

```
13   CONTINUE
9    CONTINUE
##   COMPUTE AND PRINT RESPONSE STANDARD DEVIATIONS
     WRITE(IW,107)
07   FORMAT('1'/5X, 'RESPONSE STANDARD DEVIATIONS'//5X,'NODE',6X,
    *'DISPLACEMENT',10X,'ROTATION',10X, 'ACCELERATION' /)
     IF(KD.EQ.0)GO TO 108
     USD=DSQRT(USD)
     HSD=DSQRT(HSD)
     WRITE(IW,109)USD,HSD
09   FORMAT(5X,'DAMPER', 2X, E15.5 ,21X, E15.5 )
08   CONTINUE
     J=NELEM+1
     DO 110 I=1,J
     US(I)=DSQRT(US(I) )
     VS(I)=DSQRT(VS(I) )
     HS(I)=DSQRT(HS(I) )
10   WRITE(IW,8) I,US(I),VS(I),HS(I)
     WRITE(IW,111)
111  FORMAT(/////5X,'STRAIN STANDARD DEVIATIONS'//5X, 'ELEMENTS',5X,
    *'STRAIN' / )
     DO 112 I=1,NELEM
     SS(I)=DSQRT(SS(I) )
12   WRITE(IW,14) I,SS(I)
     RETURN
     END
     FUNCTION RK(W2,G,DEPTH)
     IMPLICIT REAL*8(A-H,O-Z)
     RK=W2/G
     IF(W2.EQ.0.0) RETURN
      IF(RK*DEPTH.LT.10.0)GO TO 8
      RK=10.0/DEPTH
      RETURN
      A2=0.0
     DK=(2.0-RK)/10.0
0    A1=A2
     B=RK*DEPTH
     A2=W2-RK*G*DSINH(B) / DCOSH(B)
     IF(A2.EQ.0.0)RETURN
     RK=RK+DK
     IF(A1/A2 .GE. 0.0) GO TO 10
     RK=RK-1.5*DK
     DK=DK/2.0
2    IF(DK/RK .LT. 1.0E-4)RETURN
     B=RK*DEPTH
     A3=W2-RK*G*DSINH(B)/DCOSH(B)
     IF(A3.EQ.0.0)RETURN
     DK=DK/2.0
     IF(A3/A1 .GT. 0.0) GO TO 14
     RK=RK-DK
     A2=A3
     GO TO 12
4    RK=RK+DK
     A1=A3
     GO TO 12
     END
```

```
      FUNCTION DCOSH(A)
      IMPLICIT REAL*8(A-H,O-Z)
      B=DEXP(A)
      DCOSH=0.5*(B + 1.0/B)
      RETURN
      END
      FUNCTION DSINH(A)
      IMPLICIT REAL*8(A-H,O-Z)
      B=DEXP(A)
      DSINH=0.5*(B-1.0/B)
      RETURN
      END
      SUBROUTINE SUBP(N,A1,A2,LENGHT,ZO,DEPTH,W2,P)
      IMPLICIT REAL*8(A-H,O-Z)
      DOUBLE PRECISION MASS,LENGHT,K
      DIMENSION A(5),W(5),P(4)
      DATA A,W/0.0D0,-0.538469D0,0.538469D0,-0.906180D0,0.906180D0 ,
     *0.568889D0,2*0.478629D0,2*0.236927D0/
      DATA CI,RO,G /2.0D0,1.0D0,9.81D0 /
      K=RK (W2, G, DEPTH)
      DO 1 I=1,4
      P(I)=0.0
      Z1=ZO + LENGHT * DFLOAT(N-1)
      B=K*DEPTH
      C=3.1415926 * CI * RO * W2 / DSINH(B          )
      DO 2 I=1,5
      X=A(I)
      X=0.5 * (X+1.0)
      RADIUS = A1 * (1.0 - X) + A2 * X
      Z=Z1 + LENGHT * X
      IF(Z.GT.DEPTH)RETURN
      B=K*Z
      F=C* RADIUS **2 * DCOSH(B   ) * W(I) / 2.0*LENGHT
      H=X*X*(3.0-2.0*X)
      P(1)=P(1) + (1.0-H)*F
      P(2) =P(2) + (X * LENGHT * (1.0 - 2.0*X + X*X )) * F
      P(3)=P(3) + H*F
      P(4)=P(4) + X*X*LENGHT*(X-1.0)*F
      CONTINUE
      RETURN
      END
      SUBROUTINE SOLVE(IO,IW,NEQ,MBW,NLS,A,B,LIM,NELEM,RET,RIT,LENGHT,
     *DA,DB,S)
      IMPLICIT REAL*8(A-H,O-Z)
      DOUBLE PRECISION MASS,LENGHT
      COMPLEX*16 A,B,C,D
      DIMENSION A(1),B(15)
      DIMENSION S(1)
##    REDUCTION OF A. ORIGINAL ARRAY IS DESTROYED
      IF(IO.EQ.2)GO TO 20
      NRD=NEQ-1
      DO 18 I=1,NRD
      D=A(I)
      IF(CDABS(D).EQ. 0.0D0)GO TO 18
      IJ=I
      DO 16 J=2,MBW
```

```
      IJ=IJ+NEQ
      IF(CDABS(A(IJ)) .EQ. 0.0D0)GO TO 16
      C=A(IJ)/D
      IK=IJ
      JK=I+J-1
      DO 14 K=J,MBW
      A(JK)=A(JK)-C*A(IK)
      IK=IK+NEQ
      JK=JK+NEQ
     |CONTINUE
     |CONTINUE
      IF(IO.EQ.1)RETURN

!#    REDUCTION OF B. ORIGINAL ARRAY IS DESTROYED
      NRE=NEQ-1
      DO 26 I=1,NRE
      D=A(I)
      IF(CDABS(D).EQ.0.0D0)GO TO 26
      IJ=I
      DO 24 J=2,MBW
      IJ=IJ+NEQ
      IF(CDABS(A(IJ)).EQ.0.0D0)GO TO 24
      C=A(IJ)/D
      IK=I
      JK=I+J-1
      DO 22 K=1,NLS
      B(JK)=B(JK)-C*B(IK)
      IK=IK+NEQ
2     JK=JK+NEQ
4     CONTINUE
6     CONTINUE

##    BACKSUBSTITUTION
      I=NEQ
0     IF (CDABS(A(I)).EQ.0.0D0)GO TO 34
      IK=I
      DO 32 K=1,NLS
      B(IK)=B(IK)/A(I)
2     IK=IK+NEQ
4     I=I-1
      IF(I.EQ.0)GO TO 40
      IJ=I
      DO 38 J=2,MBW
      IJ=IJ+NEQ
      IF(CDABS(A(IJ)).EQ. 0.0D0)GO TO 38
      IK=I
      JK=I+J-1
      DO 36 K=1,NLS
      B(IK)=B(IK) - A(IJ) * B(JK)
      IK=IK+NEQ
6     JK=JK+NEQ
8     CONTINUE
      GO TO 30
##    SOLVE FOR STRAINS
0     I=(NELEM + 1)*2
      DO 39 K=1,NELEM
```

```
      J=NELEM - K +1
      N=K-1
      D=RET+(DFLOAT(N)*DA)+(DA/2.0)- RIT -(DFLOAT(N)*DB) - (DB/2.0)
      S(J)=CDABS((B(I)-B(I-2)))* D/(2.0*LENGHT)
      I=I-2
9     CONTINUE
      RETURN
      END
```

```
****** SAMPLE DATA ********

EEL-JACKETED OFFSHORE PLATFORM - 305M IN DEPTH
 4 -31    1    0   -1    0    0
   366.0        0.0      33.75        9.0       33.6        8.9      305.0
390000.0       1.83
  0.0302     0.0043      0.015
  4180.0  2432760.0
  7.2874     2.6963      1.0020390000.0      0.0500       0.03
   0.030      0.830      0.040      2.300      0.050      4.000      0.060
   0.070      3.000      0.080      2.400      0.090      2.000      0.100
   0.110      1.300      0.120      0.950      0.130      0.700      0.140
   0.150      0.340      0.160      0.295      0.170      0.250      0.180
   0.190      0.195      0.200      0.170      0.210      0.150      0.220
   0.230      0.110      0.240      0.098      0.250      0.090      0.260
   0.270      0.090      0.280      0.095      0.290      0.098      0.300
   0.310      0.095      0.320      0.095      0.330      0.095
```

```
*******************************************************************************
  This program is an extension of Program FLUID and FREQMOD of Shaaban and Nash,
  and Balendra and Nash, for the free vibration analysis of ground-supported liquid
  storage tanks.  In this work, the application is extended to elevated liquid
  storage tanks.
*******************************************************************************

      DIMENSION FS( 5000),SC(25,50),SCT(50,25),ADM(50,50)
      DIMENSION NHARMC(10)
      DATA MMD/25/,NDFSD/50/,LINEAR/ 5000/
C CARD 1
      READ 701 ,NN,MM
C     NN=NO. OF FLUID ELEMENTS ALONG THE RADIUS
C    MM=NO. OF FLU9D&ELEMENTS ALONG THE GENERATOR
  701 FORMAT(2I5)
C CARD 2
      READ 702,DENF,R,WH
  702 FORMAT(3F10.4)
C CARD 3
      READ 602, NHC
  602 FORMAT(5I5)
C CARD 4
      READ 602, (NHARMC(I),I=1,NHC)
      PRINT 200,NN,MM
  200 FORMAT(/,5X,'NO OF ELEMENTS IN THE RADIAL DIRECTION=',I5,/,5X,
     $'NO OF ELEMENTS IN THE AXIAL DIRECTION=',I5)
      PRINT 100,DENF,R,WH
  100 FORMAT(/,5X,'DENSITY OF FLUID=',E10.4,/,5X,'RADIUS OF CYLINDER=',
     $E10.4,/,5X,'HEIGHT OF FLUID=',E10.4)
      DENF=DENF/384.0
      REWIND 10
      DO 60 IHC=1,NHC
      NHR=NHARMC(IHC)
C INDEX=1 CORRESPONDS TO ASYSYMMETRIC DEFORMATION THAT IS NHR=1,3,5
      INDEX=1
      RES=NHR-(NHR/2)*2
C INDEX=2 CORRESPONDS TO SYMMETRIC DEFORMATION THAT IS NHR=0,2,4
      IF(RES .EQ. 0.) INDEX=2
      IBAND=MM+2
      NDFS=MM*2
      IF( INDEX .EQ. 1) NDFF=(NN)*MM
      IF( INDEX .EQ. 2) NDFF=(NN+1)*MM
      PRINT 1111
 1111 FORMAT(1H1)
      PRINT 300,IBAND,NDFS,NDFF
  300 FORMAT(5X,'IBAND=',I5,5X,'NDFS=',I5,5X,'NDFF=',I5,/)
      XM=FLOAT(NHR)
               CALL FLGEN(DENF,R,WH,XM,NN,MM,NDFS,IBAND,MMD,NDFSD,LINEAR,
     Q FS,SC,INDEX)
      DO 10 I=1,MM
      DO 10 J=1,NDFS
   10 SCT(J,I)=SC(I,J)
      CALL BINV(FS,SC,NDFF,IBAND,NDFS,MM,NDFSD,MMD)
C     NOW SC=FS INV *SC
      PRINT 1
C     SCT * FS INV *SC =ADM
```

```
      DO 20 I=1,NDFS
      DO 20 J=1,NDFS
      ADM(I,J)=0.0
      DO 20 K=1,MM
   20 ADM(I,J)=ADM(I,J)+SCT(I,K)*SC(K,J)
      PRINT 1
    1 FORMAT(25(2H**))
      WRITE(10) NHR
      WRITE(10) NDFS
      WRITE(10)((ADM(I,J),J=1,NDFS),I=1,NDFS)
      PRINT 17, NHR
   17 FORMAT(30X, 'ADDED MASS MATRIX FOR CIRCUMFERENTIAL WAVE=',I4)
      PRINT 11,((ADM(I,J),J=1,NDFS),I=1,NDFS)
   11 FORMAT(10(2X,E10.4))
   60 CONTINUE
      REWIND 10
      CALL FREMOD
      STOP
      END
       SUBROUTINE FLGEN(DENF,R,WH,XM,NN,MM,NDFS,IBAND,MMD,NDFSD,LINEAR,
     Q FS,SC,INDEX)
      DIMENSION FS(LINEAR),            SC(MMD,NDFSD)
      DIMENSION FK(4,4),FF(2,4),N(4)
      DX=R/FLOAT(NN)
      DY=WH/FLOAT(MM)
      A=DX*0.5
      B=DY*0.5
      DO 10 I=1,LINEAR
   10 FS(I)=0.0
      TRANSFORMATION FROM A SQUARE MATRIX TO A BANDED MATRIX
      (K,L) = (K,J)   , J=L-K+1
      TRANSFORMATION FROM A BAND TO A LINEAR ARRAY
      LFS=(K-1)*IBAND +J
      NN1=NN-1
      MM1=MM-1
      IF(INDEX .EQ. 1) NNX=NN-1
      IF(INDEX .EQ. 2) NNX=NN
      DO 1000 I=1,NNX
      IF(INDEX .EQ. 1) XO=FLOAT(I)*DX+A
      IF(INDEX .EQ. 2) XO=FLOAT(I-1)*DX+A
      CALL FSTIF(A,B,XO,FK,XM,DENF)
      DO 1000 J=1,MM1
      N(1)=(I-1)*MM+J
      N(2)=I*MM+J
      N(3)=N(2)+1
      N(4)=N(1)+1
      DO 55 II=1,4
      K=N(II)
      IPAST=K*IBAND-IBAND
      DO 51 JJ=1,4
      IF(N(JJ) .LT. N(II) ) GO TO 51
      L=N(JJ)-K+1
      LFS=IPAST+L
      FS  (LFS)=FS  (LFS)+FK(II,JJ)
   51 CONTINUE
   55 CONTINUE
```

```
000  CONTINUE
     DO 1010 I=1,NNX
     IF(INDEX .EQ. 1) XO=FLOAT(I)*DX+A
     IF(INDEX .EQ. 2) XO=FLOAT(I-1)*DX+A
     CALL FSTIF(A,B,XO,FK,XM,DENF)
     N(1)=I*MM
     N(2)=(I+1)*MM
     DO 65 II=1,2
     K=N(II)
     IPAST=K*IBAND-IBAND
     DO 61 JJ=1,2
      IF(N(JJ) .LT. N(II) ) GO TO 61
     L=N(JJ)-K+1
     LFS=IPAST+L
     FS(LFS)=FS(LFS)+FK(II,JJ)
 61  CONTINUE
 65  CONTINUE
010  CONTINUE
     IF(INDEX .EQ. 2) GO TO 76
     XO=A
     CALL FSTIF(A,B,XO,FK,XM,DENF)
     DO 1020 J=1,MM1
     N(2)=J
     N(3)=J+1
     DO 75 II=2,3
     K=N(II)
     IPAST=IBAND*K-IBAND
     DO 71 JJ=2,3
      IF(N(JJ) .LT. N(II) ) GO TO 71
     L=N(JJ)-K+1
     LFS=IPAST+L
     FS(LFS)=FS(LFS)+FK(II,JJ)
 71  CONTINUE
 75  CONTINUE
020  CONTINUE
     J=MM
     IPAST=J*IBAND-IBAND
     LFS=IPAST+1
     FS(LFS)=FS(LFS)+FK(2,2)
 76  DO 40 I=1,MMD
     DO 40 J=1,NDFSD
 40  SC(I,J)=0.0
     CALL FFORCE(R,B,FF)
     DO 3000 J=1,MM1
     NI=(J-1)*2
     DO 205 JJ=1,4
     L=NI+JJ
     SC(J,L)= SC(J,L)+FF(1,JJ)
205  SC(J+1,L)= SC(J+1,L)+FF(2,JJ)
000  CONTINUE
     NI=(MM-1)*2
     SC(MM,NI+1)=SC(MM,NI+1)+FF(1,1)
     SC(MM,NI+2)=SC(MM,NI+2)+FF(1,2)
     RETURN
     END
     SUBROUTINE BINV(A,B,NN,NB,NEQ,MM,NEQD,MMD)
```

```
      DIMENSION A(1),B(MMD,NEQD),C(35),D(1000)
      ND=NN-MM
      N=0
    5  N=N+1
      NL=(N-1)*NB
      IF(ABS(A(NL+1)).LT. 1.0E-10) A(NL+1)=1.0
       IF(N .LE. ND) GO TO 16
      NCON=N-ND
      DO 15 IB=1,NEQ
   .5 B(NCON,IB)=B(NCON,IB)/A(NL+1)
    6 CONTINUE
       IF(N .EQ. NN) GO TO 45
       DO 10 K=2,NB
      C(K)=A(NL+K)
   .0 A(NL+K)=A(NL+K)/A(NL+1)
       DO 30 L=2,NB
       I=N+L-1
       IF(NN .LT. I) GO TO 30
      J=0
      IL=(I-1)*NB
       DO 20 K=L,NB
       J=J+1
   20 A(IL+J)=A(IL+J)-C(L)*A(NL+K)
       IF(N .LE. ND) GO TO 26
      ICON=I-ND
      DO 25 IB=1,NEQ
   25 B(ICON,IB)=B(ICON,IB)-C(L)*B(NCON,IB)
   26 CONTINUE
   30  CONTINUE
       GO TO 5
      N= NO. OF EQU.
      L= NO. OF UNKNOWN
      K= SEQUENTIAL NO. OF UNKNOWN IN THE BAND
      NL+K=LFS ... LINEAR SEQUENCE
   45 DO  100 IB=1,NEQ
      DO 70 II=1,MM
   70 D(II+ND)=B(II,IB)
      DO 75 II=1,ND
   75 D(II)=0.0
      N=NN
   40 N=N-1
      NL=(N-1)*NB
      IF( N .EQ. 0) GO TO 60
      DO 50 K=2,NB
      L=N+K-1
      IF( NN.LT. L) GO TO 50
      D(N)=D(N)-A(NL+K)*D(L)
   50 CONTINUE
      GO TO 40
   60 CONTINUE
      DO 80 II=1,MM
   80 B(II,IB)=D(II+ND)
   00 CONTINUE
      RETURN
      END
      SUBROUTINE FFORCE(R,B,FF)
```

```
      DIMENSION FF(2,4)
      PI=3.14159
      DO 10 I=1,2
      DO 10 J=1,4
 10    FF(I,J)=0.0
      V=PI*R*B
      BV=V*B
      FF(1,1)=0.7*V
      FF(1,2)=BV/5.0
      FF(1,3)=0.3*V
      FF(1,4)=-2.0*BV/15.0
      FF(2,1)=0.3*V
      FF(2,2)=2.0*BV/15.0
      FF(2,3)=0.7*V
      FF(2,4)=-BV/5.0
      RETURN
      END
      SUBROUTINE FSTIF(A,B,XO,FK,XM,DENF)
       DIMENSION A1(4,4),A2(4,4),A3(4,4),FK(4,4)
       DO 12 I=1,4
       DO 12 J=1,4
      A1(I,J)=0.
      A2(I,J)=0.
2     A3(I,J)=0.
      V1=XO*B/A/6.
      A1(1,1)=2.*V1
      A1(2,2)=2.*V1
      A1(3,3)=2.*V1
      A1(4,4)=2.*V1
      A1(1,2)=-2.0*V1
      A1(2,1)=-2.0*V1
      A1(3,4)=-2.0*V1
      A1(4,3)=-2.0*V1
      A1(1,3)=-1.0*V1
      A1(3,1)=-1.0*V1
      A1(2,4)=-1.0*V1
      A1(4,2)=-1.0*V1
      A1(2,3)=V1
      A1(3,2)=V1
      A1(1,4)=V1
      A1(4,1)=V1
   2   V2=XO*A/B/6.
       A2(1,1)           =(2.-A/XO)*V2
              A2(4,4)=(2.-A/XO)*V2
      A2(1,3)=-V2
      A2(3,1)=-V2
      A2(2,4)=-V2
      A2(4,2)=-V2
       A2(2,2)           =(2.+A/XO)*V2
              A2(3,3)=(2.+A/XO)*V2
       A2(1,4)           =-(2.-A/XO)*V2
              A2(4,1)=-(2.-A/XO)*V2
       A2(2,3)           =-(2.+A/XO)*V2
              A2(3,2)=-(2.+A/XO)*V2
      A2(1,2)=V2
      A2(2,1)=V2
```

```
      A2(3,4)=V2
      A2(4,3)=V2
    3 V3=B/A/A/12.
      IF(A .EQ. XO) XO=XO+.001
      E1=((A+XO)*(A+XO)*ALOG((XO+A)/(XO-A))-2.*A*(2.*A+XO))*V3
      E2=((A-XO)*(A-XO)*ALOG((XO+A)/(XO-A))+2.*A*(2.*A-XO))*V3
      E3=((A-XO)*(A+XO)*ALOG((XO+A)/(XO-A))+2.*A*XO)*V3
      IF(A .EQ. XO) XO=XO-.001
      A3(1,1)=2.*E1
      A3(4,4)=2.*E1
      A3(2,2)=2.*E2
      A3(3,3)=2.*E2
      A3(1,2)=2.*E3
      A3(2,1)=2.*E3
      A3(3,4)=2.*E3
      A3(4,3)=2.*E3
      A3(1,3)=E3
      A3(3,1)=E3
      A3(2,4)=E3
      A3(4,2)=E3
       A3(1,4)          =E1
               A3(4,1)=E1
       A3(2,3)          =E2
               A3(3,2)=E2
      DO 10 I=1,4
      DO 10 J=1,4
   10 FK(I,J)=3.14159*(A1(I,J)+A2(I,J)+A3(I,J)*XM*XM)/DENF
      RETURN
      END
      SUBROUTINE FREMOD

      COMMON/CONST/NH,NELEMS,NNODES,NSIZE,NEQ
      COMMON/ADD/FLUIDH,NHC
      COMMON/BC/NBC
      COMMON/WE/LOWEST
      DIMENSION   FNU1(50),FNU2(50),E1(50),E2(50),G(50),T(50),SINE(51),
     $COSINE(51),SINM(50),COSM(50),R(50),PH(50), PHP(50),ARCL(50)
      DIMENSION AL(167), CHECK(8,8),RO(51),Z(51),COMENT(20),JUNK(20)
      DIMENSION D(144,145),GA( 920),IHARM(5)
      INTEGER CLFR,CLCL,CLSM
      DATA CLFR,CLCL,CLSM/'CLFR','CLCL','CLSM'/
CARD 1
      READ 5,NT,NMODE
    5 FORMAT(5I5)
CARD 2
      READ 6,FLUIDH,NHC,NHARM,LOWEST
      FORMAT(F10.4,I5,I5,I5)
CARD 3
      READ 5,(IHARM(I),I=1,NHARM)
CARD 4
      READ 7,NBC
    7 FORMAT(A4)
      REWIND NT
      READ(NT) NCARDS,JUNK
      IF(NCARDS.EQ.0.0) GO TO120
      DO110 K=1,NCARDS
```

```
 10 READ(NT)(COMENT(J),J=1,20)
    PRINT 401,(COMENT(J),J=1,20)
 01 FORMAT(2X,20A4)
 20 READ(NT) NHP,NELEMS,JUNK
    DO140 II=1,NELEMS
    READ(NT)((CHECK(I,J),I=1,8),J=1,8),(AL(I),I=1,166)
 40 CONTINUE
    NNODES=NELEMS+1
    NEQ=4*NNODES
    READ(NT)(FNU1(I),I=1,NELEMS),(FNU2(I),I=1,NELEMS),(E1(I),I=1,NELEM
   $S),(E2(I),I=1,NELEMS),(G(I),I=1,NELEMS),(T(I),I=1,NELEMS)
    DO 404 I=1,NELEMS
    PRINT 402,FNU1(I),FNU2(I),E1(I),E2(I),G(I),T(I)
402 FORMAT(2F8.3,3E12.3,E13.4)
404 CONTINUE
    DO160 I=1,NELEMS
    IF(I.EQ.NELEMS) GO TO150
    READ(NT) R(I),PH(I),PHP(I),ARCL(I),SINE(I),COSINE(I)
    GO TO160
150 READ(NT) R(I),PH(I),PHP(I),ARCL(I),SINE(I),COSINE(I),SINE(I+1),
   $ COSINE(I+1)
160 CONTINUE
    READ(NT) (RO(I),I=1,NNODES),(Z(I),I=1,NNODES)
    DO170 I=1,NELEMS
    COSM(I)=COS(PH(I))
    SINM(I)=SIN(PH(I))
170 CONTINUE
    NSIZE=10+26*NELEMS
    DO 180 IH=1,NHP
    DO 172 JH=1,NHARM
    IF(IH-1.EQ.IHARM(JH)) GO TO 175
172 CONTINUE
    READ(NT) (GA(I),I=1,NSIZE)
    READ(NT)(GA(I),I=1,NSIZE)
    GO TO 180
175 PRINT 176   , IHARM(JH)
176 FORMAT(/,2X,'CIRCUMFERENTIAL WAVE=',I5)
    NH=IHARM(JH)
    CALL AMSMAT(D,NT)
5   FORMAT(1X,12(1X,E9.2))
    NO=NEQ-4
    CALL EIGEN(D,NO,NMODE)
180 CONTINUE
    RETURN
    END
    SUBROUTINE AMSMAT(D,NT)
    COMMON/CONST/NH,NELEMS,NNODES,NSIZE,NEQ
    COMMON/ADD/FLUIDH,NHC
    DIMENSION D(144,145),BSX(920),BMX(920)
    READ(NT)(BSX(I),I=1,NSIZE)
    READ(NT)(BMX(I),I=1,NSIZE)
    DO 1 I=1,NEQ
    DO 1 J=1,NEQ
  1 D(I,J)=0.0
    CALL ADDMASS(D,BMX)
    NEQ1=NEQ+1
```

```
      DO 6 I=1,NEQ
      I1=I+1
      DO 6 J=I1,NEQ1
    6 D(I,J)=0.0
      M=0
      DO 2 I=1,8
      DO 2 J=1,I
      M=M+1
      D(J,I+1)=BSX(M)
    2 CONTINUE
      L=5
      K=0
      DO 3 I=9,NEQ
      DO 4 J=L,I
      M=M+1
      D(J,I+1)=BSX(M)
    4 CONTINUE
      K=K+1
      IF(K.NE.4) GO TO 3
      L=L+4
      K=0
    3 CONTINUE
      IF(M.NE.NSIZE) STOP
      RETURN
      END
      SUBROUTINE ADDMASS(D,BMX)
      COMMON/CONST/NH,NELEMS,NNODES,NSIZE,NEQ
      COMMON/ADD/FLUIDH,NHC
      COMMON/WE/LOWEST
      DIMENSION D(144,145),ADM(50,50) , BMX(920)
      IF(FLUIDH.EQ.0.0) GO TO 80
      REWIND 10
      DO 50 I=1,NHC
      READ(10) NHR
      READ(10) NDFS
      READ(10)((ADM(K,J),J=1,NDFS),K=1,NDFS)
      IF(NHR.EQ.NH) GO TO 80
   50 CONTINUE
      PRINT 60,NH
   60 FORMAT(2X,'ADDED MASS MATRIX FOR CIRCUMFERENTIAL WAVE=',I5,'IS NOT
     $ FOUND')
      STOP
   80 K=1
      DO 90 I=1,8
      DO 90 J=1,I
      D(I,J)=BMX(K)
      K=K+1
   90 CONTINUE
      L=5
            M=0
      DO 100 I=9,NEQ
      DO 110 J=L,I
      D(I,J)=BMX(K)
  110 K=K+1
      M=M+1
      IF(M.NE.4) GO TO 100
```

```
   L=L+4
            M=0
)0 CONTINUE
   IF(FLUIDH.NE.0.0) GO TO 25
   DO 24 I=1,NEQ
   DO 24 J=1,I
24 D(J,I)=D(I,J)
   IF(NH.NE.1)RETURN
   REWIND 11
   WRITE(11)((D(I,J),J=1,NEQ),I=1,NEQ)
   REWIND 13
   WRITE(13)((D(I,J),J=1,NEQ),I=1,NEQ)
   REWIND 13
   RETURN
DDING THE ADM MATRIX WITH SHELL MASS MATRIX AUX.
   NWET=LOWEST+1
   L=NWET
            L1=L+1
   DO 6 I=1,NDFS,2
     I2=4*L-1
     N=1
   DO 5 J=1,I,2
   J2=(L1-N)*4-1
   I21=I2+1
   J21=J2+1
   TEMP=I2
   TEMPJ=J2
   IF(I2.GT.J2) GO TO 11
   I2=J2
   J2=TEMP
11 D(I2,J2)=D(I2,J2)+ADM(I,J)
   I2=TEMP
   J2=TEMPJ
   TEMP=I21
   TEMPJ=J2
   IF(I21.GT.J2) GO TO 12
   I21=J2
   J2=TEMP
12 D(I21,J2)=D(I21,J2)+ADM(I+1,J)
   I21=TEMP
   J2=TEMPJ
   TEMP=I21
   TEMPJ=J21
   IF(I21.GT.J21) GO TO 13
   I21=J21
   J21=TEMP
13 D(I21,J21)=D(I21,J21)+ADM(I+1,J+1)
   I21=TEMP
   J21=TEMPJ
   IF(J.EQ.I) GO TO 15
   TEMP=I2
   TEMPJ=J21
   IF(I2.GT.J21) GO TO 14
   I2=J21
   J21=TEMP
14 D(I2,J21)=D(I2,J21)+ADM(I,J+1)
```

```
      I2=TEMP
      J21=TEMPJ
   15 N=N+1
    5 CONTINUE
      L=L-1
    6 CONTINUE
      DO 16 I=1,NEQ
      DO 16 J=1,I
   16 D(J,I)=D(I,J)
C IF IT IS DESIRED TO DETERMINE THE RESPONSE OF THE FLUID SOLID SYSTEM
C DUE TO BASE EXCITATION THEN MATRIX AUX FOR NAR=1 MUST BE SAVED IN TAPE
      IF(NHR.NE.1) GO TO 120
      REWIND 11
      WRITE(11)((D(I,J),J=1,NEQ),I=1,NEQ)
      REWIND 11
      REWIND 13
      WRITE(13)((D(I,J),J=1,NEQ),I=1,NEQ)
      REWIND 13
  120 CONTINUE
      RETURN
      END
      SUBROUTINE EIGEN(D,ND,NMODE)
      COMMON/BC/NBC
      DIMENSION D(144,145),V1(144),V2(144)
     $,X(140,10),OMEGA(10)
      INTEGER CLFR,CLCL,CLSM
      DATA CLFR,CLCL,CLSM/'CLFR','CLCL','CLSM'/
C      PRE-EIGENVALUE CHOLESKY REDUCTIONS
      INA=1
              ND1=ND+1
      DO 76 MA=1,ND
      DO 76 MAS=MA,ND
              MA1=MA+1
              MAS1=MAS+1
              GASH=D(MA,MAS1)
              GISH=D(MAS,MA)
              MASH=1
 79     IF(MA-MASH) 77,77,78
 78     GASH=GASH-D(MASH,MA1)*D(MASH,MAS1)
              GISH=GISH-D(MA,MASH)*D(MAS,MASH)
              MASH=MASH+1
        GO TO 79
 77     IF(MAS-MA) 81,81,119
 81     IF(GISH) 118,82,82
118     GISH=0.
 82     IF(GASH) 83,84,84
 83     GASH=0.
 84     DIAG1=SQRT(GASH)
              DIAG2=SQRT(GISH)
        IF(DIAG1.EQ.0.) GO TO 85
119     D(MA,MAS1)=GASH/DIAG1
 85     IF(DIAG2.EQ.0.) GO TO 86
              D(MAS,MA)=GISH/DIAG2
 86      CONTINUE
 76     CONTINUE
C       FORM U/UL
```

```
   DO 87 MA=1,ND
 DO 87 MAS=MA,ND
      MAS1=MAS+1
      GASH=D(MAS,MA)
      MASH=MA
   MASH=MASH+1
   IF(MAS-MASH) 88,89,89
   GASH=GASH-D(MA,MASH)*D(MASH-1,MAS1)
   GO TO 91
   D(MA,MAS1)=GASH/D(MAS,MAS1)
    CONTINUE
   MULTIPLICATION TO GET (U*ULE-1*ULTE-1*UT)
   DO 92 MA=1,ND
   DO 92 MAS=MA,ND
      MAS1=MAS+1
      GASH=0.
   DO 93 MASH=MAS1,ND1
      GASH=GASH+D(MA,MASH)*D(MAS,MASH)
3   CONTINUE
      D(MA,MAS1)=GASH
2   CONTINUE
      MODE=NMODE
   PU 1.0 IN V1 FROM 1 TO ND AND ITERATIVE
5  DO 94 I=1,ND
4  V1(I)=1.
      NUMIT=1
1  ALAM2=0.
   DO 95 I=1,ND
      I1=I+1
      GASH=0.
   DO 96 J=1,I
      GASH=GASH+V1(J)*D(J,I1)
6   CONTINUE
   IF(I-ND) 97,98,98
7  DO 99 J=I1,ND
      GASH=GASH+V1(J)*D(I,J+1)
9   CONTINUE
8  V2(I)=GASH
      ALAM2=ALAM2+GASH*GASH
5  CONTINUE
      ALAMB=SQRT(ALAM2)
      SIGSQ=0.
   DO 101 I=1,ND
      GASH=V2(I)/ALAMB
      GAS=V1(I)-GASH
      SIGSQ=SIGSQ+GAS*GAS
      V1(I)=GASH
1   CONTINUE
      ZT=1./10.**12
      NUMIT=NUMIT+1
 IF(SIGSQ-ZT)102,102,103
3   IF(NUMIT-200) 121,102,102
2   CONTINUE
    PRINT 11
   PRINT 104,NUMIT
4  FORMAT('    NO OF ITERATIONS=',I3,/)
```

```
      TO MULTIPLY (UE-1)*(U*X)
         I=ND
109   GASH=V1(I)
         J=ND
107   IF(J-I) 105,105,106
106   GASH=GASH-V2(J)*D(J,I)
         J=J-1
      GO TO 107
105   V2(I)=GASH/D(I,I)
         I=I-1
      IF(I) 108,108,109
108  PRINT 995,INA
      OMEGA IN CYCLE/SEC
    OMEGA(INA)=SQRT(1./ALAMB)/2./3.1415927
    PRINT 112 ,OMEGA(INA)
    RES=0.0
     PRINT 12
  1 FORMAT(4E14.8)
    INODE=1
200 DO 300 I=1,ND,4
    PRINT 111,INODE,V2(I),V2(I+1),V2(I+2),V2(I+3)
    INODE=INODE+1
300 CONTINUE
111 FORMAT(2X,I5,5X,E16.8,5X,E16.8,5X,E16.8,5X,E16.8)
    DO 210 I=1,ND
    X(I,INA)=V2(I)
210 CONTINUE
260 PRINT 111,INODE,RES,RES,RES,RES
      DO 113 I=1,ND
       DO 113 J=I,ND
         J1=J+1
113   D(I,J1)=D(I,J1)-ALAMB*V1(I)*V1(J)
     INA=INA+1
         MODE=MODE-1
      CHANGING TO NEXT MODE
      IF(MODE) 114,114,115
114 REWIND 14
    IF(NBC.EQ.  CLCL)ND=ND+4
    IF(NBC.EQ.  CLSM)ND=ND+3
    WRITE(14)NMODE
    DO 116 K=1,NMODE
    WRITE(14) K,OMEGA(K)
    DO 116 J=1,ND,4
    WRITE(14) X(J,K),X(J+1,K),X(J+2,K),X(J+3,K)
116 CONTINUE
    REWIND 14
     RETURN
995 FORMAT(//,10X,'MODE NO.=',I3)
 11 FORMAT(//,20X,25(2H--))
 12 FORMAT(30X,'MODE SHAPE',/,2X,'NODE',15X,'U',20X,'V',20X,'W',20X,'D
   $W/DZ')
112  FORMAT(//,10X,'NATURAL FREQUENCY=',E20.10,'IN CYCLES/SEC.')
  2 FORMAT(8E16.8)
    END
GO.FT10F001 DD UNIT=SYSDA,SPACE=(CYL,(1,1))
GO.FT11F001 DD UNIT=SYSDA,SPACE=(CYL,(1,1))
```

```
GO.FT12F001 DD DSN=F3011600.DATSA2,UNIT=DISK,
 VOL=SER=MUN003,DISP=OLD
GO.FT13F001 DD DSN=F3011600.DATMT4,UNIT=DISK,
 VOL=SER=MUN003,DISP=(NEW,KEEP),LABEL=RETPD=300,
 SPACE=(TRK,(20,10),RLSE)
GO.FT14F001 DD DSN=F3011600.DATFR4,UNIT=DISK,
 VOL=SER=MUN003,DISP=(NEW,KEEP),LABEL=RETPD=300,
 SPACE=(TRK,(20,10),RLSE)
GO.SYSIN DD *
  6    3
035885   280.0         150.0
  1
  1
 12     8
   150.0     1     1    16
  1
FR
```

```
*******************************************************************************************
   This program is an extension of Program RESPONSE of Shaaban and Nash, and Balendra
   and Nash, for the response analysis of cylindrical ground-supported liquid storage
   tanks subject to earthquake excitation.  In this work damping effects of the
   structural system is included.
*******************************************************************************************
```

```
      COMMON/GEOM/FNU1(50),FNU2(50),E1(50),E2(50),G(50),T(50),SINE(51),
     $COSINE(51),SINM(50),COSM(50),R(50),PH(50), PHP(50),ARCL(50)
      COMMON/CHALS/AL(167),CHECK(8,8)
      COMMON/THETAS/THETA(20),NTHETA
      COMMON/HARM/NHP,IHARM(5)
      COMMON/RZ/RO(51),Z(51)
      COMMON/CONST/NH,NELEMS,NNODES,NSIZE,NEQ
      COMMON/US/U(204)
      DIMENSION D(144,145),BSTF(140,4),STBB(4,4),BMASS(140,4),BBM(4,4),
     $X(140,10),UME(50),GM(10,10)
     $,BACC(4),EFFM(140,4),GP(50),PEF(140),PIN(50),SUM1(50),SUM2(50)
     $,UDD(144),A(50),ADD(50),BDIS(4),FB1(4),FB2(4),FB3(4),FB(4)
     $,GA(2001 ),COMENT(20),JUNK(20)
      DIMENSION AD(10),UD(144),RCRD(10),FB4(4),BDMP(140,4),OMED(10)
      DIMENSION FREQ(2,2),ENVRSE(2,2),COEF(2)
      DIMENSION SUM(10)
ARD 1
```

```
    READ 10,NT,RADIUS
NT IS THE TAPE IN WHICH THE STIFFNESS AND MASS MATRICES OF THE SHELL
ARE STORED BY SAMMSOR
 10 FORMAT(I5,F10.4)
ARD 2
    READ 20,ND1,ND2,ND3
 20 FORMAT(5I5)
ARD 3
    READ 30,NTHETA
 30 FORMAT(I5)
CARD 4
    READ  40,(THETA(I),I=1,NTHETA)
 40 FORMAT(8F10.4)
CARD 5
    READ 50,NH,(IHARM(I),I=1,NH)
 50 FORMAT(2I5)
CARD 6
    READ  60,PEAK,TTOTAL,DT
 60 FORMAT(3F10.4)
CARD 7
    READ  70,TSTART,TEND,TDT
 70 FORMAT(3F10.4)
    REWIND NT
    READ(NT) NCARDS,JUNK
    IF(NCARDS.EQ.0.0) GO TO120
    DO110 K=1,NCARDS
110 READ(NT)(COMENT(J),J=1,20)
    PRINT 115,(COMENT(J),J=1,20)
115 FORMAT(2X,20A4)
120 READ(NT) NHP,NELEMS,JUNK
    PI=3.14159
    RAD=PI/180.0
    DO130 I=1,NTHETA
    THETA(I)=THETA(I)*RAD
130 CONTINUE
    DO140 II=1,NELEMS
    READ(NT)((CHECK(I,J),I=1,8),J=1,8),(AL(I),I=1,166)
140 CONTINUE
    NNODES=NELEMS+1
    NEQ=4*NNODES
    READ(NT)(FNU1(I),I=1,NELEMS),(FNU2(I),I=1,NELEMS),(E1(I),I=1,NELEM
   $S),(E2(I),I=1,NELEMS),(G(I),I=1,NELEMS),(T(I),I=1,NELEMS)
    DO160 I=1,NELEMS
    IF(I.EQ.NELEMS) GO TO150
    READ(NT) R(I),PH(I),PHP(I),ARCL(I),SINE(I),COSINE(I)
    GO TO160
150 READ(NT) R(I),PH(I),PHP(I),ARCL(I),SINE(I),COSINE(I),SINE(I+1),
   $ COSINE(I+1)
160 CONTINUE
    READ(NT) (RO(I),I=1,NNODES),(Z(I),I=1,NNODES)
    DO170 I=1,NELEMS
    COSM(I)=COS(PH(I))
    SINM(I)=SIN(PH(I))
170 CONTINUE
    NSIZE=10+26*NELEMS
SINCE ONLY HAR=1 WILL BE EXCITED MUST SKIP K $ M MATRICES OF HAR=0
```

```
      READ(NT) (GA(I),I=1,NSIZE)
      READ(NT)(GA(I),I=1,NSIZE)
      CALL EXTR CT(D,NEQ,NT)
      READ(13) N3,N4,NFREE
      READING THE FREQUENCIES $ MODES FOR HARMONIC=1 FROM TEPE 14
       REWIND 14
      READ(14) NEV
      DO 180 I=1,NEV
      READ(14) K,OME(I)
 CONVERTING THE FREQUENCIES INTO RAD/SEC.
      OME(I)=OME(I)*2.0*PI
      DO 180 J=1,N4,4
      READ(14)   X(J,I),X(J+1,I),X(J+2,I),X(J+3,I)
180   CONTINUE
      REWIND 14
      READ(13)((D(I,J),J=1,N4),I=1,N4)
NOW D IS THE K MATRIX OF NON BASE NODES
<B IS DENOTED AS BSTF
      READ(13) ((BSTF(I,J),J=1,4),I=1,N4)
<BB IS DENOTED AS STBB
      READ(13) ((STBB(I,J),J=1,4),I=1,4)
      READ(13)((D(I,J),J=1,N4),I=1,N4)
NOW D IS THE M MATRIX OF NON BASE NODES
MB IS DENOTED AS BMASS
      READ(13)((BMASS(I,J),J=1,4),I=1,N4)
MBB IS DENOTED AS BBM
      READ(13) ((BBM(I,J),J=1,4),I=1,4)
      REWIND 13
      READ 2,(RCRD(I),I=1,NEV)
      FORMAT(10F8.4)
      DO 77 J=1,NEV
7     OMED(J)=OME(J)*SQRT(1.0-RCRD(J)*RCRD(J))
      FREQ(1,1)=1.0/OME(1)
      FREQ(1,2)=OME(1)
      FREQ(2,1)=1.0/OME(2)
      FREQ(2,2)=OME(2)
      DET=FREQ(1,1)*FREQ(2,2)-FREQ(2,1)*FREQ(1,2)
       ENVRSE(1,1)=FREQ(2,2)/DET
       ENVRSE(1,2)=-FREQ(1,2)/DET
       ENVRSE(2,2)=FREQ(1,1)/DET
       ENVRSE(2,1)=-FREQ(2,1)/DET
      COEF(1)=2.0 * (ENVRSE(1,1)*RCRD(1) + ENVRSE(1,2)*RCRD(2) )
      COEF(2)=2.0 * (ENVRSE(2,1)*RCRD(1) + ENVRSE(2,2)*RCRD(2) )
      DO 3110 I=1,N4
      DO 3110 J=1,4
110   BDMP(I,J)=COEF(1)*BMASS(I,J)+COEF(2)*BSTF(I,J)
      PRINT 3,COEF(1),COEF(2)
      FORMAT(1X,2F20.10)
      CALL MODAN(D,X,GM,N4,NEV)
      DO 200 I=1,4
      DO 190 K=1,N4,4
      BBM(I,1)=BBM(I,1)+BMASS(K,I)
      BBM(I,2)=BBM(I,2)+BMASS(K+1,I)
      BBM(I,3)=BBM(I,3)+BMASS(K+2,I)
      BBM(I,4)=BBM(I,4)+BMASS(K+3,I)
190   CONTINUE
```

```
00 CONTINUE
   CALL EFFM SS(D,BMASS,N4,EFFM)
   NTIME=TTOTAL/DT+1.0001
EAK IS G=384.0 IN/SEC/SEC
CCELERATIONS ARE NORMALIZED BY G
HE ACCELERATION RECORD GENERATED BY PSEQGN IS STORED IN TAPE 20
   REWIND 9
   READ(9)(GA(I),I=1,NTIME)
1  FORMAT(8F9.6)
   REWIND 9
05 FORMAT(10E10.4)
   PRINT 210,TTOTAL
10 FORMAT(/,10X,'TANK IS EXCITED BY AN ARTIFICIAL EARTH QUAKE APPLIED
  $FOR',F10.4,'SEC.',/)
   PRINT 215,PEAK
15 FORMAT(//,10X,'MAX.GROUND ACCELERATION=',F10.4,'IN./SEC/SEC',/)
   BACC(1)=0.0
   BACC(2)=-PEAK
   BACC(3)=PEAK
   BACC(4)=0.0
   DO220 I=1,N4
   PEF(I)=0.0
   DO220 J=1,4
20 PEF(I)=PEF(I)+EFFM(I,J)*BACC(J)
   DO230 I=1,NEV
   SUM1(I)=0.0
   SUM2(I)=0.0
   SUM(I)=0.0
   GP(I)=0.0
   DO230 J=1,N4
230 GP(I)=GP(I)+X(J,I)*PEF(J)
   NSTART=TSTART/DT + 1.0001
   NEND=TEND/DT+1.0001
   NDT=TDT/DT
   DPLM X1=0.0
   DPLM X2=0.0
   DPLM X3=0.0
   ISTART=2
   REWIND 8
   REWIND 9
   REWIND 10
   WRITE(8) TDT
   WRITE(9)TDT
   WRITE(10)TDT
   DO 320 IT=NSTART,NEND,NDT
   ITIME=IT-1
   TIME=FLOAT(ITIME)*DT
    CALL DUHAML(GA,GP,TIME,ITIME,DT,NEV,OME,OMED,RCRD,PIN,AD,GM,SUM,
  *ISTART)
   ISTART=IT
A IS THE DISPLACEMENT IN MODAL COORDINATES
J IS THE NODAL DISPLACEMENTS
ADD IS THE ACC.  IN MODAL COORDINATES
JDD IS THE ACC OF THE NON BASE NODES
   DO270 I=1,NEV
   A(I)=PIN(I)/(GM(I,I)*OMED(I) )
```

```
 270   ADD(I)=GP(I)*GA(IT)/GM(I,I)-OME(I)*OME(I)*A(I)-2.0*OME(I)*RCRD(I)*
      1AD(I)
       DO 275 I=1,NEQ
       U(I)=0.
       UD(I)=0.
       UDD(I)=0.0
 275   CONTINUE
       DO280 I=1,N4
       DO280 J=1,NEV
       U(I)=U(I)+X(I,J)*A(J)
       UD(I)=UD(I) + X(I,J)*AD(J)
       UDD(I)=UDD(I)+X(I,J)*ADD(J)
  280  CONTINUE
       IF(ABS(DPLM X1).GT.ABS(U(ND1))) GO TO 291
       DPLM X1=U(ND1)
       TMEM X1=TIME
C 291 WRITE(8) U(ND1)
 291   CONTINUE
       IF(ABS(DPLM X2).GT.ABS(U(ND2)))GO TO 292
       DPLM X2=U(ND2)
       TMEM X2=TIME
C 292 WRITE(9) U(ND2)
 292   CONTINUE
       IF(ABS(DPLM X3).GT.ABS(U(ND3)))GO TO 293
       DPLM X3=U(ND3)
       TMEM X3=TIME
C293   WRITE(10)U(ND3)
 293   CONTINUE
C BASE REACTIONS
       BACC(1)=0.0
       BACC(2)=-PEAK*GA(IT)
       BACC(3)=PEAK*GA(IT)
       BACC(4)=0.0
C FB1=MBT*UDD
C FB2=KBT*U
C FB3=(MBB+MBT*I)*BACC
C FB=FB1+FB2+FB3 IS THE BASE REACTION
       DO 310 I=1,4
       FB1(I)=0.
       FB2(I)=0.
       FB3(I)=0.
       FB4(I)=0.
       DO 300 J=1,N4
       FB1(I)=FB1(I)+BMASS(J,I)*UDD(J)
       FB4(I)=FB4(I) + BDMP(J,I)*UD(J)
       IF(J.GT.4)GO TO 300
       JK=N4-4+J
       FB2(I)=FB2(I)+BSTF(JK,I)*U(JK)
       FB3(I)=FB3(I)+BBM(I,J)*BACC(J)
  300  CONTINUE
 305   FB(I)=( FB1(I)+FB2(I)+FB3(I)+FB4(I) ) / (PI*RADIUS)
  310  CONTINUE
       CALL PRINT(TIME,U,FB,N4,NEQ)
       CALL STRESS
  320  CONTINUE
C      REWIND 8
```

```
C     REWIND 9
C     REWIND 10
      PRINT 510,ND1,DPLM X1,TMEM X1
      PRINT 510,ND2,DPLM X2,TMEM X2
      PRINT 510,ND3,DPLM X3,TMEM X3
  510 FORMAT(//,2X,'THE MAXIMUM VALUE OF THE DEGREE OF FREEDOM',I4,'=',
     $E12.4,'OCCURES AT',F10.4,'SEC')
      RETURN
      END
      SUBROUTINE EXTR CT(D,NEQ,NT)
      DIMENSION D(144,145)
      NFREE=NEQ
      N4=NFREE-4
      N3=NFREE-3
      REWIND 13
      WRITE(13) N3,N4,NFREE
      CALL READ RY(D,NT)
C PARTIONING THE STIFFNESS MATRIX
C  WRITING K MATRIX IN TAPE15
      WRITE(13)((D(I,J),J=1,N4),I=1,N4)
C WRITE KB
      WRITE(13)((D(I,J),J=N3,NFREE),I=1,N4)
C WRITE KBB
      WRITE(13)((D(I,J),J=N3,NFREE),I=N3,NFREE)
      REWIND NT
C READING THE MODIFIED MASS MATRIX  (M+ADM)
      REWIND 11
      READ(11)((D(I,J),J=1,NEQ),I=1,NEQ)
C  WRITE M
      WRITE(13)((D(I,J),J=1,N4),I=1,N4)
C WRITE MB
      WRITE(13)((D(I,J),J=N3,NFREE),I=1,N4)
C WRITE MBB
      WRITE(13)((D(I,J),J=N3,NFREE),I=N3,NFREE)
      REWIND 13
      RETURN
      END
      SUBROUTINE READ RY(D,NT)
C READING THE STIFFNESS MATRIX STORED IN TAPE NT
      COMMON/CONST/NH,NELEMS,NNODES,NSIZE,NEQ
      DIMENSION D(144,145),BX(920)
      NFREE=NEQ
      DO 1 I=1,NFREE
      DO 1 J=1,NFREE
    1 D(I,J)=0.0
C READS AN ARRAY INTO A SQUARE MATRIX
      READ(NT)(BX(I),I=1,NSIZE)
      M=0
      DO 2 I=1,8
      DO 2 J=1,I
      M=M+1
      D(I,J)=BX(M)
    2 D(J,I)=D(I,J)
      L=5
      K=0
      DO 3 I=9,NFREE
```

```
      DO 4 J=L,I
      M=M+1
      D(I,J)=BX(M)
    4 D(J,I)=D(I,J)
      K=K+1
      IF(K.NE.4) GO TO 3
      L=L+4
      K=0
    3 CONTINUE
      IF(M.NE.NSIZE)STOP
      RETURN
      END
      SUBROUTINE MODAN(D,X,GM,N4,NEV)
      DIMENSION D(144,145),X(140,10),XM(140,10),GM(10,10)
      DO 10 I=1,N4
      DO 10 J=1,NEV
      XM(I,J)=0.0
      DO 10 K=1,N4
      XM(I,J)=XM(I,J)+D(I,K)*X(K,J)
   10 CONTINUE
C B=XT*A*X
      DO 20 I=1,NEV
      DO 20 J=1,NEV
      GM(I,J)=0.0
      DO 20 K=1,N4
      GM(I,J)=GM(I,J)+X(K,I)*XM(K,J)
   20 CONTINUE
      RETURN
      END
      SUBROUTINE EFFM SS(D,BMASS,N4,EFFM)
      DIMENSION D(144,145),EFFM(140,4) ,BMASS(140,4)
C DIS THE MASS MATRIX OF NON BASE NODES
C  TO FORM MI MATRIX
      DO 10 I=1,N4
      DO 10 J=1,4
   10 EFFM(I,J)=0.0
      DO 20 I=1,N4
      DO 20 K=1,N4,4
      EFFM(I,1)=EFFM(I,1)+D(I,K)
      EFFM(I,2)=EFFM(I,2)+D(I,K+1)
      EFFM(I,3)=EFFM(I,3)+D(I,K+2)
      EFFM(I,4)=EFFM(I,4)+D(I,K+3)
   20 CONTINUE
      DO 30 I=1,N4
      DO 30 J=1,4
      EFFM(I,J)=-(EFFM(I,J)+EMASS(I,J))
   30 CONTINUE
      RETURN
      END
      SUBROUTINE DUHAML(GA,GP,TIME,NT,DT,M,OME,OMED,RCRD,PIN,AD,GM,SUM,
     *ISTART)
      DIMENSION GA(2001 ),GP(10),OME(10),RCRD(10),PIN(10),AD(10)
     *,GM(10,10),OMED(10)
      DIMENSION SUM(10)
      DIMENSION SINE(10),EXPO(10)
      DO 15 J=1,M
```

```
      DO 10 IT=ISTART,NT
      TA=FLOAT(IT)*DT
      SINE(J)=SIN( OMED(J)* (TIME-TA))
      EXPO(J)=EXP ( -RCRD(J) * OME(J) * (TIME-TA))
      SUM(J)=SUM(J) + GA(IT) * EXPO(J) * SINE(J)
      IF(IT.EQ.NT)AD(J)=GA(IT)*EXPO(J)*SINE(J)*GP(J)/(GM(J,J)*OMED(J))
10    CONTINUE
15    PIN(J)=SUM(J)*GP(J)*DT
      RETURN
      END
      SUBROUTINE PRINT(T,U,FB,N4,NEQ)
      DIMENSION U(204),FB(4)
      PRINT 100,T
 100  FORMAT(20X,25(2H--),/,15X,'TIME=',F10.4,/)
      PRINT 200
 200  FORMAT(/,2X,'NODE',10X,'U',18X,'V',18X,'W',14X,'DW/DZ')
      RES=0.0
      JK=1
      DO 240 I=1,NEQ,4
      IF(JK.NE.15)GO TO 239
      IF(JK.EQ.15)WRITE(7,245)U(I+2)
245   FORMAT(E20.5)
      PRINT 250,JK,U(I),U(I+1),U(I+2),U(I+3)
239   CONTINUE
      IF(JK.NE.17)GO TO 240
      PRINT 250,JK,U(I),U(I+1),U(I+2),U(I+3)
 240  JK=JK+1
 250  FORMAT(3X,I3,5X,E12.4,5X,E12.4,5X,E12.4,5X,E12.4)
      PRINT 400
 400  FORMAT(/,25X,'REACTION AT THE BASE',/)
      PRINT 500,FB(1),FB(2),FB(3),FB(4)
 500  FORMAT(10X,'AXIAL FORCE(NS)=',E12.4,'POUND/INCH',/,4X,'TANGENTIAL
     $FORCE(NST)=',E12.4,'POUND/ INCH',/,9X,'RADIAL FORCE(NR)=',E12.4,'PO
     $UND/INCH',/,9X,'AXIAL MOMENT(MS)=',E12.4,'POUND INCH/INCH')
      RETURN
      END
      SUBROUTINE STRESS
      COMMON/EES/ES(5),ET(5),EST(5),E13(5),E23(5)
      COMMON/CONST/NH,NELEMS,NNODES,NSIZE,NEQ
      COMMON/THETAS/THETA(20),NTHETA
      COMMON/HARM/NHP,IHARM(5)
      COMMON/GEOM/FNU1(50),FNU2(50),E1(50),E2(50),G(50),T(50),SINE(51),
     $COSINE(51),SINM(50),COSM(50),R(50),PH(50), PHP(50),ARCL(50)
      COMMON/GCD/CC1,CC2,DD1,DD2,GG1,GG2
      COMMON/US/U(204)
      PRINT 100
      DO 200 I1=1,NELEMS
      CALL STRAIN(I1)
      DO 400 I=1,NTHETA
      ESU=0.0
      ETU=0.0
      ESTU=0.0
      E13U=0.0
      E23U=0.0
      CHIS=0.0
      CHIT=0.0
```

```
      CHIST=0.0
      CTHIS=0.0
      CTHIT=0.0
      CTHIST=0.0
      XIH1=IHARM(IH)
      CS=COS(XIH1*THETA(I))
      SN=SIN(XIH1*THETA(I))
      K=4*(I1-1)+NEQ*(IH-1)
C CALCULATION OF LINEAR STRAIN
      ESU=ESU+ES(IH)*CS
      ETU=ETU+ET(IH)*CS
      ESTU=ESTU+EST(IH)*SN
      E13U=E13U+E13(IH)*CS
      E23U=E23U+E23(IH)*SN
C CALCULATION OF CHANGE OF CURVATURE
      UB3=-U(K+1)*SINE(I1)+U(K+3)*COSINE(I1)
      UB7=-U(K+5)*SINE(I1+1)+U(K+7)*COSINE(I1+1)
      CHIS1=(U(K+4)-U(K+8))/ARCL(I1)
      CHIS=CHIS+CHIS1*CS
      CHIT1=(-XIH1*E23(IH)-SINM(I1)*E13(IH))/R(I1)
      CHIT=CHIT+CHIT1*CS
      CHIST1=(XIH1*E13(IH)+SINM(I1)*E23(IH)-XIH1*SINM(I1)*(UB3+UB7)/
     $(2.*R(I1))+XIH1*(UB7-UB3)/ARCL(I1)+(U(K+6)-U(K+2))*COSM(I1)/ARCL(I
     $1)-(U(K+6)+U(K+2))*SINM(I1)*(COSM(I1)/(2.*R(I1))+PHP(I1)/2.))/R(I1
     $)
      CHIST=CHIST+CHIST1*SN
      CTHIS=CTHIS+XIH1*CHIS1*(-SN)
      CTHIT=CTHIT+XIH1*CHIT1*(-SN)
      CTHIST=CTHIST+XIH1*CHIST1*CS
  500 CONTINUE
C  CALCULATION OF MID SURFACE STRAINS
      EPS=ESU
      EPT=ETU
      EPST=ESTU
C CALCULATION OF STRESS $ MMOMENT RESULTANTS
      STRNS=CC1*EPS+FNU1(I1)*CC1*EPT
      STRNT=FNU2(I1)*CC2*EPS+CC2*EPT
      STRNST=GG1*EPST
      STRMS=DD1*CHIS+FNU1(I1)*DD1*CHIT
      STRMT=FNU2(I1)*DD2*CHIS+DD2*CHIT
      STRMST=GG2*CHIST
      THETA1=THETA(I)*180./3.14159
      IF(I1.NE.15)GO TO 399
      IF(I1.EQ.15)WRITE(7,300)STRMS
  300 FORMAT(E20.5)
      PRINT 700,I1,THETA1,STRNS,STRNT,STRNST ,STRMS,STRMT,STRMST
  399 CONTINUE
      IF(I1.NE.17)GO TO 400
      PRINT 700,I1,THETA1,STRNS,STRNT,STRNST ,STRMS,STRMT,STRMST
  400 CONTINUE
  200 CONTINUE
  100 FORMAT(//,25X,'FORCE RESULTANTS',26X,'MOMENT RESULTANTS'
     $  ,/,19X,'N(S)',10X,'N(T)',8 X,'N(ST)',10X,'M(S)', 8X,'M(T)',10X,'
     $M(ST)',//,1X,'ELEM THETA',/,1X,'NO',4X,'(DEG)')
  700 FORMAT(I4,F8.4,6(1X,E12.4))
  900 FORMAT(I4,F8.4,8(1X,E12.4))
```

```
      RETURN
      END
      SUBROUTINE STRAIN(I1)
      COMMON/CONST/NH,NELEMS,NNODES,NSIZE,NEQ
      COMMON/HARM/NHP,IHARM(5)
      COMMON/EES/ES(5),ET(5),EST(5),E13(5),E23(5)
      COMMON/GEOM/FNU1(50),FNU2(50),E1(50),E2(50),G(50),T(50),SINE(51),
     $COSINE(51),SINM(50),COSM(50),R(50),PH(50), PHP(50),ARCL(50)
      COMMON/RZ/RO(51),Z(51)
      COMMON/US/U(204)
      COMMON/GCD/CC1,CC2,DD1,DD2,GG1,GG2
      DIMENSION E23Q1(5),E23Q3(5),E23Q5(5),E23Q7(5),ESTQ1(5),ESTQ3(5),
     $ ESTQ5(5),ESTQ7(5),ETQ2(5),ETQ6(5)
C COMPUTES STRAINS FOR AN ELEMENT
C WRITEN FOR ANY HARMONIC ASSUMING THE DISPLACEMENTS ARE ARRANGED IN A S
C  ROW FROM HARMONIC=0 TO HARMONIC=NH
C IN PROGRAM RESP  ONLY HARMONIC=1  IS EXCITED THUS THE ARRAY U HAS DISP
C  HARMONIC=1 ONLY
      FN=1.-FNU1(I1)*FNU2(I1)
      CC1=E1(I1)*T(I1)/FN
      CC2=E2(I1)*T(I1)/FN
      GG1=G(I1)*T(I1)
      GG2=G(I1)*T(I1)**3./12.0
      DD1=E1(I1)*T(I1)**3./(12.*FN)
      DD2=E2(I1)*T(I1)**3./(12.*FN)
      J1=I1
      J11=I1+1
      DRO=RO(J11)-RO(J1)
      DZ=Z(J11)-Z(J1)
      ARL=SQRT(DRO*DRO+DZ*DZ)
      SIPH=DRO/ARL
      COPH=DZ/ARL
      RM=(RO(J1)+RO(J11))/2.0
      R2I=1.0/(2.0*RM)
      ARCLI=1.0/ARL
      ETQ3=R2I
      ETQ7=R2I
      E23Q2=-R2I*COPH
      E23Q6=E23Q2
      E13Q1=ARCLI*SIPH
      E13Q3=-ARCLI*COPH
      E13Q5=-ARCLI*SIPH
      E13Q7=ARCLI*COPH
      ESTQ2=-SIPH*R2I-ARCLI
      ESTQ6=-SIPH*R2I+ARCLI
      ESQ1=E13Q3
      ESQ3=-E13Q1
      ESQ5=E13Q7
      ESQ7=-E13Q5
      CO2R=COPH*R2I
      SL2R=SIPH*R2I
      CL2R=COPH*R2I
      SO2R=SIPH*R2I
      DO 300 IH=1,NH
      K=IHARM(IH)
      XK=K
```

```
      E23Q1(IH)=SO2R*XK
      E23Q3(IH)=-CO2R*XK
      E23Q5(IH)=SL2R*XK
      E23Q7(IH)=-CL2R*XK
      ESTQ1(IH)=E23Q3(IH)
      ESTQ3(IH)=-E23Q1(IH)
      ESTQ5(IH)=E23Q7(IH)
      ESTQ7(IH)=-E23Q5(IH)
      ETQ2(IH)=R2I*XK
      ETQ6(IH)=ETQ2(IH)
C COMPUTE ET,ES,EST,E13, E23
      KK=NEQ*(IH-1)+4*(I1-1)
      KK1=KK+1
      KK2=KK+2
      KK3=KK+3
      KK5=KK+5
      KK6=KK+6
      KK7=KK+7
      ET(IH)=ETQ2(IH)*U(KK2)+ETQ3*U(KK3)+ETQ6(IH)*U(KK6)+ETQ7*U(KK7)
      ES(IH)=ESQ1*U(KK1)+ESQ3*U(KK3)+ESQ5*U(KK5)+ESQ7*U(KK7)
      EST(IH)=ESTQ1(IH)*U(KK1)+ESTQ2*U(KK2)+ESTQ3(IH)*U(KK3)+ESTQ5(IH)*U
     $(KK5)+ESTQ6*U(KK6)+ESTQ7(IH)*U(KK7)
      E13(IH)=E13Q1*U(KK1)+E13Q3*U(KK3)+E13Q5*U(KK5)+E13Q7*U(KK7)
      E23(IH)=E23Q1(IH)*U(KK1)+E23Q2*U(KK2)+E23Q3(IH)*U(KK3)+E23Q5(IH)*U
     $(KK5)+E23Q6*U(KK6)+E23Q7(IH)*U(KK7)
  300 CONTINUE
      RETURN
      END
//GO.FT09F001 DD DSN=F3011600.INPT3,UNIT=DISK,
// VOL=SER=MUN004,DISP=OLD
//GO.FT12F001 DD DSN=F3011600.DATSA2,UNIT=DISK,
// VOL=SER=MUN003,DISP=OLD
//GO.FT11F001 DD DSN=F3011600.DATMT5,UNIT=DISK,
// VOL=SER=MUN003,DISP=OLD
//GO.FT13F001 DD UNIT=SYSDA,SPACE=(CYL,(1,1))
//GO.FT14F001 DD DSN=F3011600.DATFR5,UNIT=DISK,
// VOL=SER=MUN003,DISP=OLD
//GO.SYSIN DD *
   12    280.000
   51    63   127
    1
    0.0000
    1     1
 384.00000     12.5000      0.01
    0.1000     12.5000      0.1000
  0.0001   0.05
//
/*
```